https://doi.org/10.5194/acp-2021-69
Preprint. Discussion started: 4 February 2021

Atmospheric Chemistry and Physics Discussions

Seasonal distribution and drivers of surface fine particulate matter and organic aerosol over the Indo-Gangetic Plain

Caterina Mogno[1], Paul I. Palmer[1,2], Christoph Knote[3], Fei Yao[1], and Timothy J. Wallington[4]

[1]School of GeoSciences, University of Edinburgh, Edinburgh, UK
[2]National Centre for Earth Observation, University of Edinburgh, Edinburgh, UK
[3]Model-Based Environmental Exposure Science (MBEES), Faculty of Medicine, University of Augsburg, Germany
[4]Research & Advanced Engineering, Ford Motor Company, Dearborn, MI, 48121-2053, USA

Correspondence: Caterina Mogno (c.mogno@ed.ac.uk)

Abstract.

The Indo-Gangetic Plain (IGP) is home to 6% of the global population and is responsible for a large fraction of agricultural crop production in Pakistan, India, and Bangladesh. Levels of fine particulate matter (mean diameter <2.5 microns, $PM_{2.5}$) across the IGP often exceed human health recommendations, making cities across the IGP among the most polluted in the world. Seasonal changes in the physical environment over the IGP are dominated by the large-scale South Asian monsoon system that dictates the timing of agricultural planting and harvesting. We use the WRF-Chem model to study the seasonal anthropogenic, pyrogenic, and biogenic influences on fine particulate matter and its constituent organic aerosol (OA) over the IGP that straddles Pakistan, India, and Bangladesh during 2017/2018. We find that surface air quality during pre-monsoon (March—May) and monsoon (June—September) seasons is better than during post-monsoon (October—December) and winter (January—February) seasons, but all seasonal mean values of $PM_{2.5}$ still exceed the recommended levels, so that air pollution is a year-round problem. Anthropogenic emissions influence the magnitude and distribution of $PM_{2.5}$ and OA throughout the year, especially over urban sites, while pyrogenic emissions result in localized contributions over the central and upper parts of IGP in all non-monsoonal seasons, with the highest impact during post-monsoon seasons that correspond to the post-harvest season in the agricultural calendar. Biogenic emissions play an important role in the magnitude and distribution of $PM_{2.5}$ and OA during the monsoon season, and shows a substantial contribution to secondary OA (SOA) particularly over the lower IGP. We find that the OA contribution to $PM_{2.5}$ is significant in all four seasons (17-30%), with primary OA generally representing the larger fractional contribution. We find that the volatility distribution of SOA is driven mainly by the mean total OA loading and the washout of aerosols and gas-phase aerosol precursors that result in SOA being less volatile during the pre-monsoon and monsoon season than during the post-monsoon and winter seasons.

1 Introduction

The Indo-Gangetic Plain (IGP), including parts of Pakistan, India and Bangladesh (Figure 1), is one of the most populous and polluted areas in the world. It is home to more than 400 million people (6% of the global population) and the associated sources of air pollution, which are distributed disproportionately over cities of various sizes from megacities of more than 10 million

https://doi.org/10.5194/acp-2021-69
Preprint. Discussion started: 4 February 2021

Atmospheric Chemistry and Physics Discussions

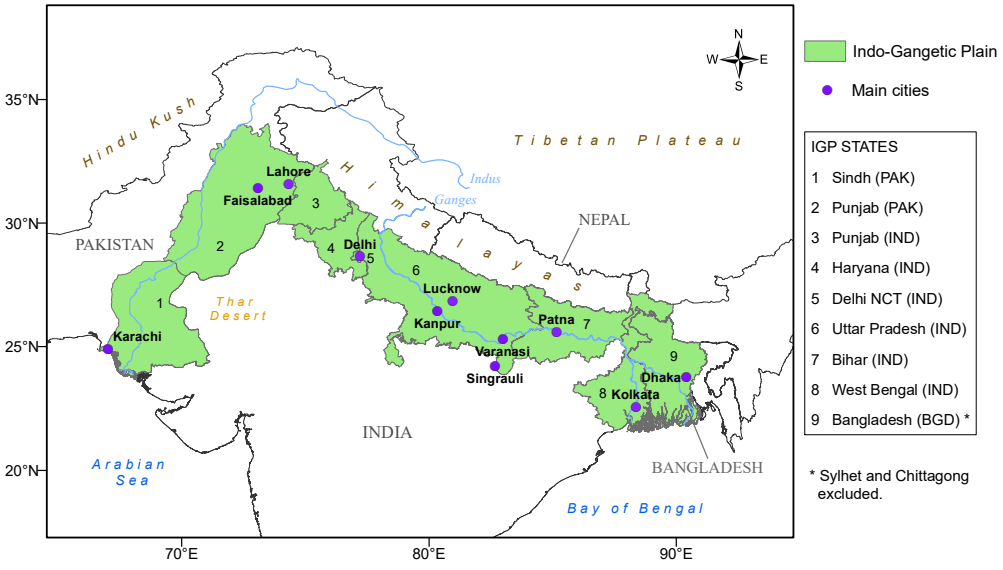

Figure 1. Geographical and administrative features of the Indo-Gangetic Plain (IGP), including Pakistan, India, and Bangladesh. Numbers denote individual IGP states and purple dots denote the main cities.

people, e.g. Karachi, Lahore, Delhi, Kolkata, and Dhaka, to smaller cities of a few million inhabitants, e.g. Faisalabad, Patna, Kanpur, Lucknow, and Varanasi (DESA, 2018). It has been estimated that there would be a potential gain in life expectancy in the IGP of approximately 4-6 years if levels of $PM_{2.5}$ were reduced to standards set by the World Health Organisation (Greenstone et al., 2020; WHO, 2016). The unique geography of the IGP and broader scale meteorological drivers, coupled with the regional diversity of seasonal pollutant emission sources makes this region one of the most challenging places to study the controls of its air pollution and the consequent impact on human health. Here, we use the WRF-Chem regional atmospheric chemistry and transport model to describe the seasonal patterns of surface organic aerosol and $PM_{2.5}$ and to help disentangle the role of anthropogenic, pyrogenic and biogenic emissions on their surface patterns across the IGP.

The importance of the IGP lies in the fertility of its soils formed from alluvium that is deposited across the Indus and Ganges basins by the Indus and Ganges rivers. These rivers originate in the Himalaya mountains and the Tibetan Plateau. The Indus and Ganges basins benefit also from precipitation from the seasonal monsoon. The monsoon timing also defines the main seasons over the IGP (India Meteorological Department): the pre-monsoon season runs from March to May, the monsoon season is from June to September, the post-monsoon season is from October to December, and winter occurs in January and February. (June to September). The Indian states across the IGP (e.g. Punjab, Haryana, and Uttar Pradesh) represent the vast majority of

https://doi.org/10.5194/acp-2021-69
Preprint. Discussion started: 4 February 2021


Atmospheric Chemistry and Physics Discussions

nationwide wheat and rice production. Rice and wheat are planted in May and November and harvested in October-November and April-May respectively, following the rice–wheat cropping cycle. The IGP is also an important producer of sugarcane, cultivated mainly in the Indus Valley in Pakistan and in the Indian state of Uttar-Pradesh. The two main seasons for planting are in September-October and February-March, followed by harvesting during the winter and pre-monsoon months, respectively. Crop residues left from harvesting, e.g. husk, bran, straw, are generally burned in open fires. Traditionally, these residues were ploughed back into the soil to maintain fertility and stability, but the sheer scale of current production precludes these practices in time for a second growing season (Chauhan et al., 2012; Ahmed et al., 2015). Open burning of these residues across the IGP, particularly during the post-monsoon season, is a large source of gaseous and particulate pollution that has implications for regional air quality and human health (Vadrevu et al., 2011; Jethva et al., 2019; Sembhi et al., 2020). Residential biofuel combustion also plays an important role for air quality (Conibear et al., 2020; Agarwala and Chandel, 2020).

The high population density and intense human activity over the IGP result in anthropogenic emissions being a major source of regional surface air pollution (Begum et al., 2013; Guttikunda and Jawahar, 2014; Shahid et al., 2015; Venkataraman et al., 2018). Residential energy consumption represents a major contribution to anthropogenic emissions with a large fraction of the rural and urban population using solid fuel for cooking (Conibear et al., 2018). Emissions from land transportation, particularly in cities, also represents a significant contribution to anthropogenic emissions (Begum et al., 2013; Guttikunda et al., 2014; Mallik and Lal, 2014). Intense agriculture over the IGP is associated with large emissions of ammonia, an aerosol precursor, from urea fertilizer application, as well as from post-harvest burning as described above (Kuttippurath et al., 2020; Wang et al., 2020). Vegetation cover over the IGP consists mainly of croplands (Stibig et al., 2007; Gumma et al., 2019), which have lower isoprene emissions than trees (Hardacre et al., 2013). Consequently, biogenic emissions over the IGP are lower compared to other parts of South Asia (Guenther et al., 2006; Stavrakou et al., 2014).

Regional dispersion of air pollution over the IGP is dominated on a seasonal timescale by the monsoon system, influenced by the high mountain ranges of Hindu Kush and Himalayas that lie to the northwest to northeast of the IGP. Agricultural planting and harvesting (and associated burning) are determined by the timing of the monsoon when the majority of the annual rainfall falls. Consequently, observed variations of $PM_{2.5}$ reflect large-scale variations in meteorology and the seasonal variations in anthropogenic, biogenic, and pyrogenic emissions (Jethva et al., 2005; Lelieveld et al., 2018; Schnell et al., 2018).

A growing body of regional models have been used to study the relationship between emissions, meteorology, and $PM_{2.5}$ over India (Kumar et al., 2015b; Bran and Srivastava, 2017; Kulkarni et al., 2020; Ojha et al., 2020), and to estimate the health impacts of outdoor exposure to $PM_{2.5}$ (Ghude et al., 2016; Conibear et al., 2018; David et al., 2019). Many studies have focused on post-monsoon biomass burning episodes and on air pollution during the winter season over the upper-central Indian part of the IGP (Guttikunda and Gurjar, 2012; Ram et al., 2012; Pant et al., 2015; Kumar et al., 2015a; Jethva et al., 2018; Singh et al., 2018; Krishna et al., 2019; Mhawish et al., 2020). But of course the IGP also includes parts of Pakistan and Bangladesh that remain poorly studied even though they are connected via atmospheric transport. With only a few exceptions, these studies have focused on total $PM_{2.5}$ although there is evidence that single aerosol components play a major role in $PM_{2.5}$ composition over the IGP (Gani et al. (2019) and Singh et al. (2018) and references therein). Measurements have shown that organic aerosol (OA), originating from anthropogenic, pyrogenic, and biogenic emissions, constitute a significant fraction (20-35%) of $PM_{2.5}$

https://doi.org/10.5194/acp-2021-69
Preprint. Discussion started: 4 February 2021


Atmospheric Chemistry and Physics Discussions

across the IGP especially during post-monsoon and winter seasons (Ram et al., 2008; Alam et al., 2014; Rajput et al., 2014; Behera and Sharma, 2015; Sharma et al., 2016). OA exists as a complex mixture, comprising of thousands of individual organic compounds, and it is made up of primary OA (POA), emitted directly to the atmosphere, and of secondary OA (SOA) formed by the condensation of organic vapours as they become progressively less volatile through oxidation (Seinfeld and Pandis, 2016; Donahue et al., 2006). Changes in OA volatility is key for the formation of SOA, and it is particularly sensitive to temperature, ambient concentration of OA, and nitrogen oxide levels (Shrivastava et al., 2017). We take advantage of the Volatility Basis Set (VBS) model, which helps to describe succinctly the evolving volatility of OA through oxidative chemistry in the atmosphere (Donahue et al., 2006, 2012; Chuang and Donahue, 2016), described below. This method has been used successfully in a range of modelling studies (Lane et al., 2008b; Bergström et al., 2012; Ahmadov et al., 2012; Zhang et al., 2013; Zhao et al., 2016).

We use the WRF-Chem regional atmospheric chemistry model to characterise the seasonal and spatial distributions and composition of $PM_{2.5}$ and OA in light of synoptic meteorology and emission drivers over three sub-regions of the IGP, including relevant parts of Pakistan and Bangladesh. We use a 1-D VBS model to describe the evolution of OA and its influence on $PM_{2.5}$, described in section 2. In section 2, we also describe the *in situ* and satellite measurements we use to evaluate our model. In section 3, we describe the seasonal meteorology over the IGP, the seasonal distributions and composition of $PM_{2.5}$ and OA, and the seasonal distribution of SOA volatility. In section 3 we also use a perturbative approach to understand the sensitivity of $PM_{2.5}$ constituent distributions to changes in anthropogenic, pyrogenic and biogenic emissions and to seasonal changes in the atmospheric environment. We conclude our study in section 4.

2 Data and Methods

Here, we describe the WRF-Chem model that we use to understand the influence of anthropogenic, pyrogenic, and biogenic emissions on the atmospheric distribution of $PM_{2.5}$ and OA over the IGP.

2.1 Weather Research and Forecasting model coupled with Chemistry

We use v.3.9.1.1 of the the Weather Research and Forecasting (WRF) model coupled with Chemistry (WRF-Chem) (Grell et al., 2005) to describe the emissions and atmospheric chemistry and transport associated with gas and aerosol phase compounds over the IGP during 2017 and 2018. WRF uses the Advanced Research WRF (ARW) dynamical solver to solve the fully compressible, non-hydrostatic Euler equations that describe atmospheric flow. These calculations are coupled with atmospheric chemistry so that that our $PM_{2.5}$ and OA calculations are consistent with the meteorology.

Our study domain is defined as 17°–40° N and 64°–97° E, encompassing the IGP at a horizontal spatial resolution of 20 km and using 33 vertical levels that span from the surface to 50 hPa ($\simeq$19 km). To define our initial conditions and lateral boundary conditions, and for nudging (Newtonian relaxation), we use meteorological reanalyses from NCEP FNL Operational Model Global Tropospheric Analyses Data (National Centers for Environmental Prediction, National Weather Service, NOAA, U.S. Department of Commerce, 2015) at a spatial resolution of $0.25° \times 0.25°$ and at a temporal resolution of six hours. We use the nudging approach at all levels to prevent our calculations from deviating too far from observed meteorology. Table A1 provides

https://doi.org/10.5194/acp-2021-69
Preprint. Discussion started: 4 February 2021

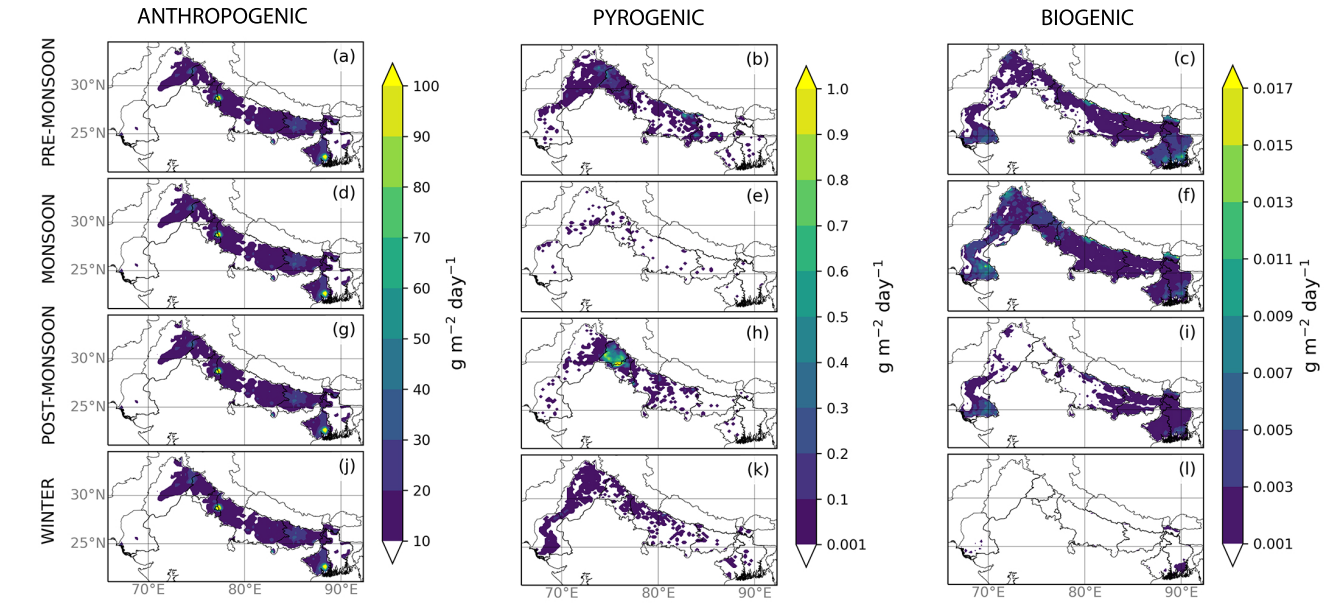

Figure 2. Seasonal mean daily emissions over the IGP (g m^{-2} day^{-1}) of (left) column) anthropogenic, (middle column) biomass burning, and (right column) biogenic (isoprene) emissions. Anthropogenic emissions from EDGAR-HTAP and fire emissions from FINN. Biogenic emissions are calculated online in WRF-Chem using MEGAN. See main text for further details.

more details about the meteorological processes we use in our calculations. Chemical initial conditions and lateral boundary conditions for each month are provided by six-hourly CAM-CHEM global model data (Buchholz et al., 2019). We spin-up each simulation for a week before studying the model output to minimize the influence of the initial conditions.

To describe gas-phase chemistry we use the Model for OZone And Related chemical Tracers, version 4 (MOZART-4) chemical mechanism (Emmons et al., 2010), including the extended treatment of volatile organic compound (VOC) chemistry (Knote et al., 2014). Photolysis rates are calculated by the Fast Tropospheric Ultraviolet–Visible (FTUV) module (Tie et al., 2003).

We use the Model for Simulating Aerosol Interactions and Chemistry (MOSAIC) to simulate aerosols chemistry (Zaveri et al., 2008), including aqueous-phase chemistry (Knote et al., 2014). MOSAIC describes aerosols using four sectional discrete size bins: 0.039—0.156μ m, 0.156—0.625μ m, 0.625—2.5μ m, 2.5–10μ m. The first three of these bins represent $PM_{2.5}$, while the largest one describes coarse particulate matter ($PM_{2.5-10}$). We use the 1-D VBS method to describe SOA for WRF-Chem (Knote et al., 2015), based on previous studies (Lane et al., 2008b; Ahmadov et al., 2012). For each of the four aerosol size bins in MOSAIC, the 1-D VBS implementation considers five volatility bins for semi-volatile organic compounds (SVOCs), described by effective saturation concentrations C* of 10^{-4}, 1, 10, 100 and 10^3 μg m^{-3} at 298 K. The $log_{10}C^* = -4$ volatility corresponds to an inert compound, and serves computationally as a loss of particle phase organics to avoid unrealistic volatile mixtures due to continuously aging of gas-phase SVOCs. Lumped anthropogenic, pyrogenic, and biogenic gas-phase aerosol

https://doi.org/10.5194/acp-2021-69
Preprint. Discussion started: 4 February 2021


Atmospheric Chemistry and Physics Discussions

precursors undergo continuous gas-phase oxidation and partition between the gas and aerosol phase using pseudo-ideal partitioning theory (Pankow, 1994). Partitioning between the gas and aerosol phase depends on total organic aerosol load and temperature. SOA yields are also dependent on NO_x levels, so SOA yields is calculated differently for low and high NO_x conditions, through a branching ratio (Lane et al., 2008a). We also include the SOA formation from glyoxal (Knote et al., 2014). Loss of SVOCs is from washout via convective and grid scale precipitation. Our chosen implementation of VBS only accounts for SVOCs, and assumes that POA is inert so that it contributes only to the aerosol mass. We do not include direct emissions of SVOCs or intermediate VOCs (IVOCs). This is a limitation of our current implementation given evidence that SVOC and IVOC vapours creates a considerable amount of regional SOA, and that POA emissions are semivolatile and undergo oxidation and should be also considered in describing SOA production (Robinson et al., 2007). To describe POA using the VBS approach we would require information about the volatility distribution of POA, but conventional inventories typically consider POA as non-volatile. Further details of this VBS implementation in WRF-Chem are described in Knote et al. (2015) and references therein.

We use monthly anthropogenic emissions from Emission Database for Global Atmospheric Research with Task Force on Hemispheric Transport of Air Pollution (EDGAR-HTAP v2.2) for year 2010 (Janssens-Maenhout et al., 2015) as provided by the WRF-Chem community, which provides the total anthropogenic emissions and includes a NMVOC speciation according to the gas and aerosol chemistry scheme we use here (MOZART-MOSAIC); hourly biomass burning emisions from the Fire Inventory from NCAR (FINN) inventory for year 2017/2018 (Wiedinmyer et al., 2011); and biogenic emissions are calculated online using the Model of Emissions of Gases and Aerosol from Nature (MEGAN, Guenther et al. (2006)).

Figure 2 shows the seasonal distributions of total anthropogenic, pyrogenic, and biogenic (predominately isoprene) emissions over the IGP. Total anthropogenic emissions have been calculated by summing the mass contribution from all the chemical species (gas and particle) specified in the inventory once preprocessed onto the model domain using the WRF-Chem tools for the community ACOM-NCAR. We converted gas emissions to mass units using the appropriate molar mass for each species. The same approach has been used to calculate fire emissions, while isoprene emissions are calculated online by MEGAN in the WRF-Chem model and then converted to mass units. Anthropogenic emissions generally dominate in all seasons (Figure 2a,d,g,j) with daily values ranging from 10^1 to 10^2g m^{-2} day^{-1}. The two largest localised regions of anthropogenic emissions are Delhi and Kolkata with emissions $>$100 g m^{-2} day^{-1}, followed by smaller indian cities, e.g. Patna, Varanasi, Kanpur and Lucknow (Figure 1). Just south of the border of Uttar-Pradesh, the Madhya Pradesh district of Singrauli hosts several large power plants. The Pakistani and Bangladeshi parts of the IGP generally have the lowest anthropogenic emissions, with the exception of Karachi in south Pakistan, the north Pakistani Punjab (the most populated part of Pakistan where Lahore and Fasibalad are located), and Dhaka in Bangladesh. Emissions from Karachi and Dhaka have lower per capita emissions than Indian cities of comparable size.

Fires have a strong seasonal cycle, peaking during pre-monsoon and post-monsoon seasons (Figure 2b,h), with emissions $\sim 10^{-1}$g m^{-2} day^{-1} mainly due to agricultural stubble burning. The post-monsoon harvesting season includes fire emissions rates that are three times higher compared to the pre-monsoon season ($\sim$ 0.3 g m^{-2} day^{-1} and $\sim$ 0.9 g m^{-2} day^{-1}, respectively). Post-monsoon fires are almost exclusively located in the Indian Punjab, with the largest values at the border with

https://doi.org/10.5194/acp-2021-69
Preprint. Discussion started: 4 February 2021


Atmospheric Chemistry and Physics Discussions

Haryana state. Pre-monsoon fires are located around the border of Pakistani and Indian Punjab and upper Haryana. There are also some isolated fires in the eastern part of the IGP. During winter (Figure 2k), low fire activity is present in the Indus valley in Pakistan and mainly over Uttar-Pradesh from post-harvesting of sugarcane crop.

Biogenic emissions peak during pre-monsoon and monsoon seasons (Figure 2c,f), with values of 2×10^{-3}g m^{-2} day^{-1} and 1.5×10^{-2}g m^{-2} day^{-1}, respectively. The largest values are over Sindh in Pakistan, West Bengal, and Bangladesh. Land cover over the IGP is dominated by croplands, but state of Sindh includes coastal mangrove plantations, inlands riverine forests, irrigated plantations, and rangelands (of Environment Government of Pakistan, 2009). Moreover, West Bengal and Bangladesh emissions are mostly confined close to the coast, where forest land is present (Reddy et al., 2016). During these two seasons there are also isoprene emissions over Uttar Pradesh from forests in Pilibhit and Kheri, and from northeast Pakistan.

For computational expediency we have chosen a representative period of one month for each distinct season over the IGP. We define, based on the seasonal definition of the Indian Meteorological Department (India Meteorological Department), the pre-monsoon period as 18th April to 16th May 2017; the monsoon season as 3rd to 31st July 2017; the post monsoon season at 18th October to 16th November 2017; and finally winter as 8th January to 5th February 2018. The 2017/2018 year is close to the climatological mean state so our results are typical of this region rather than being influenced by significant circulation changes due to, for example, El Niño Southern Oscillation climate variations (Null, 2020).

For the purposes of reporting our results we divide the IGP into three sub-regions: the upper IGP that includes the Pakistani states of Sindh and Punjab and the Indian Punjab; the middle IGP that includes the Indian states of Haryana, Delhi NCT, and Uttar Pradesh; and the lower IGP that include the Indian state of Bihar and West Bengal and Bangladesh, excluding the states of Chittagong and Sylhet (Figure 1).

2.2 Determining the Sensitivity of $PM_{2.5}$ and OA to Changes in Precursor Emissions

We use a perturbative approach to determine the importance of different source sectors on $PM_{2.5}$ and OA, which takes into account the non-linear chemical environment. Alternatively, setting a particular emission source to zero would result in a significant non-linear response that is unique to the source, consequently precluding any meaningful comparison of the importance of a particular source to $PM_{2.5}$ and OA.

First, we run a base run for each season. We then, for each season, systematically perturb one emission source by +5% over the study domain for the central week of each season, keeping the other sources the same as the base run. Finally, we calculate the sensitivity S_{ij} of species concentration C at the gridpoint ij to the changes in emissions ΔE:

$$S_{ij} = \frac{\Delta C_{ij}}{\Delta E} = \frac{\sum_t (C^p_{ij,t} - C^b_{ij,t})}{\sum_{ij,t,s} (E^p_{ij,t,s} - E^b_{ij,t,s})}, \quad (1)$$

where $C^p_{ij,t}$ and $C^b_{ij,t}$ are the concentrations of our target species ($PM_{2.5}$ and OA in this study) of the perturbed run p and base run b, respectively; $E^p_{ij,t,s}$ and $E^b_{ij,t,s}$ are the emissions of species s associated with a specific emission sector from the perturbed and base runs, respectively. Total emissions at each gridpoint ij for species s over time duration Δt is calculated by $E_{ij,t,s} = \epsilon_{ij,t,s}\Delta t A_{ij}$, where $\epsilon_{ij,t,s}$ is the species s emission rate at location ij and time t, and A_{ij} denotes the area of gridpoint ij, which in our calculations is 400 km^2. The sum of emissions ΔE in the equation denominator includes changes in

https://doi.org/10.5194/acp-2021-69
Preprint. Discussion started: 4 February 2021


Atmospheric Chemistry and Physics Discussions

emissions over the IGP. To take into account the spatial variability of emissions patterns, we weight ΔE with the total number of gridcells within the IGP that show emission difference corresponding to a mean emission rate above 0.001 g m^{-2} day^{-1} (translating to a change in cumulative emissions > 2.8 Mg for each gridcell for the one week simulation considered). This threshold corresponds to a lower limit for significant emissions rate across the area considered (Figure 2). We neglect values of S_{ij} where the change in the pollutant concentration C_{ij} <5% of mean pollutant seasonal concentration over the IGP (4 μg m^{-3} and 1 μg m^{-3} for $PM_{2.5}$ and total OA, respectively). Using this additional threshold allows us to isolate significant changes in concentrations due to direct changes in emissions, and remove smaller values due to model non-linearities. We report the sensitivity parameter S_{ij} with units of μg m^{-3} Gg^{-1}.

We perturb directly anthropogenic and fire emissions rates. Biogenic emissions are calculated online by scaling normalized emission rates by factors that describes changes in, for example, temperature, photosynthetic active radiation, leaf area index (LAI) (Guenther et al., 2006). We modify the WRF-Chem code to increment only isoprene emissions because our calculations suggest they account for almost all of biogenic emissions over the IGP, in agreement with other studies (Singh et al., 2011; Surl et al., 2018).

2.3 Data Used for Model Evaluation

We use *in situ* measurements of $PM_{2.5}$, PM_{10}, CO, NO_2, O_3, and SO_2 from the Indian Central Pollution Control Board CPCB and $PM_{2.5}$ data collected atop the US Embassy in Pakistan and Bangladesh U.S. Department of State. We accessed these data from the OpenAQ Platform (OpenAQ). Appendix B describes an overview of the *in situ* data, our data cleaning approach, and evaluation metrics. Given the lack of continuous measurements of OA and its componets POA and SOA over the IGP, we compare our model OA with measurements available from the literature. We also evaluate the model using satellite observations of aerosol optical depth (AOD) from the NASA Moderate Resolution Imaging Spectroradiometer (MODIS) instrument aboard the Terra and Aqua satellites, which have a local equatorial overpass time of 1030 and 1330, respectively. AODs are retrieved at 550 nm, corresponding to particle sizes of 0.1–2μm and comparable to the $PM_{2.5}$ size range. In particular, we use the MODIS Collection 6.1 Level 2 combined Dark Target and Deep Blue AOD product available on a 10 km spatial resolution (Levy et al., 2013).

Here we summarize the main results of our evaluation (detailed results are available in Appendix B). We report the normalized mean bias (NMB) and the Pearson correlation coefficient r, which we use to describe how well the model reproduces the observations. The model tends to overestimate surface $PM_{2.5}$ concentrations (0.004<NMB<0.4) especially during monsoon season (NMB=0.4) but it has skill in reproducing observed seasonal variations ($r > 0.62$) with the exception of the monsoon season ($r = 0.09$). For PM_{10}, the model tends to underestimate the observation in all seasons (NMB up to -0.25) except in premonsoon season (NMB=0.15) and has poorer skill in reproducing observed PM_{10} variations compared to $PM_{2.5}$ ($r \leq 0.69$), especially during winter and pre-monsoon season. We generally find poorer model agreement with gas-phase pollutants, especially O_3 and NO_2 (Table A3), which may be due to discrepancies between model and observation spatial and temporal scales. Overall, our ground-based evaluation results are in agreement with Conibear et al. (2018) who used a similar model set-up over India. For OA, the model reproduces the order-of-magnitude seasonal trends (Table A4) but additional measurements

https://doi.org/10.5194/acp-2021-69
Preprint. Discussion started: 4 February 2021


Atmospheric Chemistry and Physics Discussions

are needed to robustly assess model performance. Table A5 shows that WRF-Chem AOD agree with spatial distributions of MODIS AODs with r typically > 0.5 with the exception of the monsoon season (r=0.35). Apparent poor model skill during the monsoon season may reflect difficulties in retrieving AOD due to extensive cloud coverage during this season. The model tends to overestimate MODIS AOD during pre-monsoon (NMB=0.33, 0.26 for Terra and Aqua satellites) and slightly underestimate AOD in the other seasons (NMB ranges from -0.06 to -0.19).

3 Results

First, we summarise the seasonal meteorology over the IGP, which influences the physical and chemical environments that determine $PM_{2.5}$ and OA. We then report seasonal distributions of surface $PM_{2.5}$ and the corresponding constituent aerosol composition. Finally, we investigate the seasonal influence of POA and SOA on $PM_{2.5}$ and the volatility of the surface SOA across the IGP. In describing the seasonal distribution of $PM_{2.5}$, OA, POA and SOA we highlight the influence of anthropogenic, pyrogenic, and biogenic emissions and synoptic meteorology in shaping these patterns.

For the purpose of describing $PM_{2.5}$ and OA we begin our narrative with the post-monsoon season and finish with the monsoon season, reflecting the central importance of the monsoon system on atmospheric chemistry over the IGP. However, in the corresponding figures we retain the chronological order of events in a calendar year.

3.1 Seasonal Meteorological Drivers

Figure A1 shows model seasonal mean values for planetary boundary layer height (PBLH, m), surface relative humidity (RH, %), surface temperature (°C), mean daily rainfall (mm day^{-1}), and 10 m wind (m s^{-1}) over the IGP. Given that PBLH and RH show a diurnal cycle with high variance we report nighttime and daytime values for these variables.

During the pre-monsoon season, mean surface temperatures are higher than 30°C. Mean PBLH ranges from 1000 m up to 4500 m at daytime, with the highest values are over Pakistan and central IGP, and is almost an order of magnitude smaller during nighttime (120 m up to 400 m). Seasonal mean winds are typically 3 m s^{-1}, southward from the northern mountain chain of Hindu Kush and the Himalayas, and stronger northward from the coast, allowing pollutants to be transported mainly in the inland. Air is much more humid over the lowest part of the IGP (>60%). Rainfall follows similar patterns of RH, limited to Bangladesh with values below $\sim$3 mm day^{-1}.

During the monsoon season, the dominant feature is the monsoon itself. This manifests most obviously in increased rainfall, which increases the washout of hydrophillic pollutants, mainly in the central and lower part of the IGP, with mean daily rainfall values of 3-7 mm day^{-1} with localized regions of rainfall in excess of 15 mm day^{-1}, and wind speeds in excess of 6 m s^{-1} north-northeastward. Values of RH are $>$50% almost everywhere over the IGP, and relatively low values for the PBLH allow a well mixed chemical environment, with smaller day to night variation compared to pre-monsoon (1000-3000 m day, 500-1200 m night). Mean temperatures are similar to those during the pre-monsoon, with the most prominent increase over northern Pakistan (>35 °C).

https://doi.org/10.5194/acp-2021-69
Preprint. Discussion started: 4 February 2021

Atmospheric Chemistry and Physics Discussions

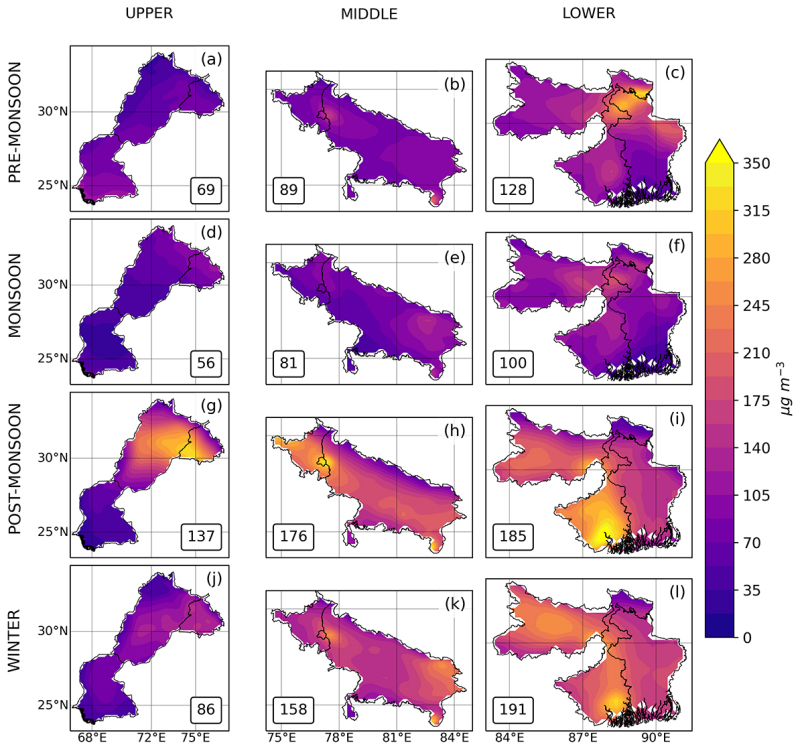

Figure 3. Seasonal mean spatial distributions of $PM_{2.5}$ (μg m^{-3}) over the upper, middle and lower IGP. The numbers inset of pre-monsoon (a–c), monsoon (d–f), post-monsoon (g–i), and winter (l–n) seasons denote the regional mean $PM_{2.5}$ value.

The post-monsoon season is characterized by cooler temperatures than the previous two seasons with mean values of ∼23°C, much lower values for PBLH (below 2000 m during day and ∼200 m during night), and weaker wind speeds (< 1 m s^{-1} with no predominant direction, a combination of factors that results in pollution stagnation. With the exception of Bangladesh and the Indian states that are adjacent to the Bay of Bengal, rainfall is almost absent from the IGP. Nevertheless, air continues to be humid with the distribution and values of RH similar to the monsoon season, with values of up to 80% over the central and lower IGP, environmental conditions that favour water significantly contributing to PM mass without washout from rain.

During winter, mean temperature further drops to ∼15°C with cooler temperatures over regions adjacent to the northern mountain chains. PBLH values are at their daily annual minimum (<∼1000 m) and its night values are similar to post-monsoon (<∼200 m). Winds speeds are typically <12 m s^{-1} with a net west-east gradient from the upper IGP to the lower IGP, which transports pollutants towards Bihar, West Bengal and Bangladesh, and with a north-south gradient over the Indus Basin that transports pollution from northern Pakistan to the coast. Daily rainfall is below 3 mm day^{-1} anywhere across the IGP, but as for post-monsoon, RH remains high over the central and lower IGP (>40% daytime, 70% during nighttime).

https://doi.org/10.5194/acp-2021-69
Preprint. Discussion started: 4 February 2021

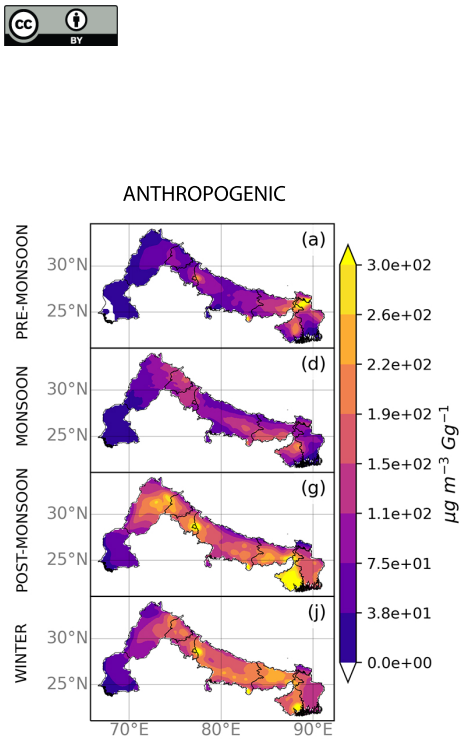

Atmospheric Chemistry and Physics Discussions
Open Access
EGU

Figure 4. Seasonal sensitivity of $PM_{2.5}$ concentrations to changes in (left column) anthropogenic, (middle column) pyrogenic, and (right column) biogenic emissions (μ g $m^{-3}Gg^{-1}$). The calculation is described in the main text. Regions marked as white denote where sensitivity corresponds to $PM_{2.5}$ concentrations below the set threshold of 4 μg m^{-3}.

3.2 Seasonal Distributions of Surface $PM_{2.5}$

Figure 3 shows seasonal variations of surface $PM_{2.5}$ across the upper, middle, and lower IGP. Generally, we find the highest values of surface $PM_{2.5}$, up to 350 μg m^{-3}, during post-monsoon and winter seasons that are associated with lower PBLH allowing large anthropogenic emissions to accumulate in the boundary layer without ventilation from strong winds. From this section we begin out narrative from the post-monsoon season and finish with the monsoon season, but retain the Figure panels in chronological order for a particular calendar year. Our seasonal distributions of $PM_{2.5}$ are similar to recent studies (Shahid et al., 2015; Ojha et al., 2020; Mhawish et al., 2020) although we report higher $PM_{2.5}$ concentrations especially over the lower IGP.

During the post-monsoon season (Figure 3 (g–i)), the mean values of surface $PM_{2.5}$ in the upper, middle, and lower IGP are 137 μg m^{-3}, 176 μg m^{-3}, and 185 μg m^{-3}, respectively. On a local scale, Kolkata and its surroundings in the lower IGP experience the worst air quality with mean $PM_{2.5}$ values in excess of 300 μg m^{-3}, closely followed by Delhi NCT, the border region between Indian and Pakistani Punjab, and Singrauli at the southern border of middle IGP ($\sim$300 μg m^{-3}). The best air quality is found in the Pakistani state of Sindh with $PM_{2.5}$ concentrations below 75 μg m^{-3}. Biomass burning in the Indian Punjab plays a key role in shaping the distribution of $PM_{2.5}$ during this season. Figure 4h shows that fire emissions have the largest impact on $PM_{2.5}$ concentrations across the Indian and Pakistani Punjab region, Haryana and Delhi NCT (sensitivities of up to 5×10^3 μg m^{-3} Gg^{-1}). Post-monsoon biomass burning emissions do not impact the central and lower IGP, where $PM_{2.5}$

https://doi.org/10.5194/acp-2021-69
Preprint. Discussion started: 4 February 2021


Atmospheric Chemistry and Physics Discussions

concentrations are more sensitive to anthropogenic emissions. The sensitivity of $PM_{2.5}$ to changes in anthropogenic emissions (Figure 4g) is similar to biomass burning over the cities of Lahore and Faisalabad in the Punjab states, and Delhi NCT. The sensitivity of $PM_{2.5}$ to changes in biogenic emissions (Figure 4i) have non-negligible values (5×10^2 μg m^{-3} Gg^{-1}) only over part of West Bengal in the lower IGP.

During the winter season (Figure 3(j–l)), wind patterns transport pollutants from the upper IGP to the lower IGP, resulting in west-east gradient in seasonal mean $PM_{2.5}$ concentrations . The mean $PM_{2.5}$ value in the lower IGP is 191 μg m^{-3}, the highest mean seasonal value for the IGP. The highest $PM_{2.5}$ concentrations are reached in Kolkata (>300 μg m^{-3}), and in the Bihar state, with a local peak in Patna (>220 μg m^{-3}) known as the 'Bihar pollution pool' (Kumar et al., 2018). In the middle IGP, mean $PM_{2.5}$ concentrations are 18 μg m^{-3} lower than post-monsoon levels, with east Delhi and Singauli remaining the largest hotspots of the region (>220 μg m^{-3}). The upper IGP experiences the lowest seasonal $PM_{2.5}$ concentration (86 μg m^{-3}), lower than half the value in the lower IGP, with concentrations decreasing from the Punjab to the Sindth coast. Anthropogenic emissions dominate the distribution of $PM_{2.5}$ during winter over central and lower IGP (sensitivity of 3.5×10^2 μg m^{-3} Gg^{-1}, Figure 4j), with the highest sensitivities over Kolkata, Singrauli, and Delhi. The influence of biomass burning is mainly limited to the the Indus basin, stretching until Uttar Pradesh (Figure 4k), while biogenic emissions do not show a significant influence during this season (Figure 4l).

During the pre-monsoon season (Figure 3 a–c), air quality begins to improve due to higher PBLHs and stronger winds (Figure A1) that help to disperse pollutants. Mean $PM_{2.5}$ concentrations are similar over the upper and middle IGP with values lower than 90 μg m^{-3}. Higher concentrations remain in the lower IGP (128 μg m^{-3}) due to the accumulation of pollutants from the winds blowing from the Bay of Bengal to the slopes of the Himalayas over North Bangladesh. $PM_{2.5}$ values over the upper part of the middle IGP (Figure3 b) show some influence from biomass burning (Figure 4 b). We find that anthropogenic emissions are most important over the lower IGP and localized region in the central IGP (Figure 4 a). $PM_{2.5}$ concentrations in Delhi NCT are jointly influenced by biomass burning and anthropogenic sources. Biogenic sources only have a significant impact over localized regions in the lower and middle IGP (Figure 4(c)).

Generally, the onset of the monsoon results in better air quality across the IGP due to higher rainfall rates, which increases wet deposition of aerosols, and higher PBLHs that improve the physical dispersal of surface emissions. Mean values of $PM_{2.5}$ are $\leq$100 μg m^{-3} across the IGP. The largest values of $PM_{2.5}$ are over the lower IGP (up to 170 μg m^{-3}). The sensitivity of $PM_{2.5}$ is highest for biogenic emissions, particularly for the upper and middle IGP. Anthropogenic emissions impact mainly the central and lower IGP and the upper part of the upper IGP. Fires play only a small role in $PM_{2.5}$ during this season.

Surface $PM_{2.5}$ composition

Figure 5 shows the composition of $PM_{2.5}$ across the IGP. Generally, we find more variability between seasons than across different parts of the IGP, except for the water contribution to $PM_{2.5}$ mass. The results we report for the chemical composition and seasonal trends of $PM_{2.5}$ are broadly consistent with chemical characterisation studies over the region (Chowdhury et al., 2007; Bhowmik et al., 2020).

https://doi.org/10.5194/acp-2021-69
Preprint. Discussion started: 4 February 2021

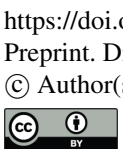

Atmospheric Chemistry and Physics Discussions

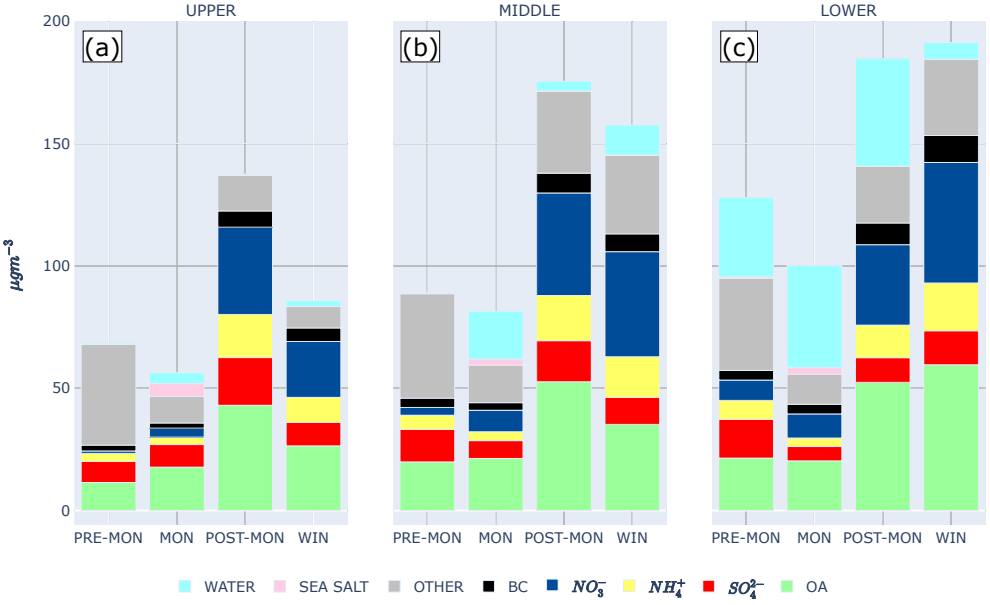

Figure 5. Seasonal mean $PM_{2.5}$ composition from the WRF-Chem model across the IGP: (a) upper, (b), middle, and (c) lower IGP. The constituents include sea salt (sum of sodium (Na) and chloride (Cl)), NH_4^+, SO_4^{2-}, NO_3^-, the sum of the remaining inorganic compounds (OTHER), total OA, BC, and liquid water.

Inorganic species (secondary inorganic aerosol of sulfate, nitrate and ammonium and other inorganic aerosol) dominate the chemical composition by mass of $PM_{2.5}$, representing between 30–80% of total $PM_{2.5}$ for each season across the IGP. The mean seasonal mass of total inorganics across the IGP is 54–70 μg m^{-3} during the pre-monsoon season, 27–35 μg m^{-3} during the monsoon season,79–111 μg m^{-3} during the post-monsoon season, and 51–114 μg m^{-3} during winter. The largest inorganic aerosol values are found during the post-monsoon and winter seasons due to nitrate from fossil fuel combustion and from residential and energy use. We find a similar but relatively muted seasonal variation for black carbon with mass values between 2–11 μg m^{-3}. Sea salt transported from the coasts during the monsoon season adds 3–5 μg m^{-3} (3–9%) to $PM_{2.5}$ across the IGP.

The water contribution to $PM_{2.5}$ is substantial over the lower IGP during pre-monsoon, monsoon, and post-monsoon seasons, with mass contribution of 32–44 μg m^{-3} (25–42%), while during winter it accounts for 6 μg m^{-3} (3.5%). For the middle IGP, water is a non-negligible fraction of $PM_{2.5}$ mainly during monsoon (20 μg m^{-3}, 24%) and winter (12 μg m^{-3}, 8%) seasons, while for the upper IGP the highest values of water mass are found during only the monsoon season (4 μg m^{-3}, 8%). The seasonal variation of water content reflects RH distritbuions, which above values of 60–70% allows PM hydrophilic components (e.g., nitrate, sulfate, sea salt) to uptake water via deliquescence.

https://doi.org/10.5194/acp-2021-69
Preprint. Discussion started: 4 February 2021

Atmospheric Chemistry and Physics Discussions

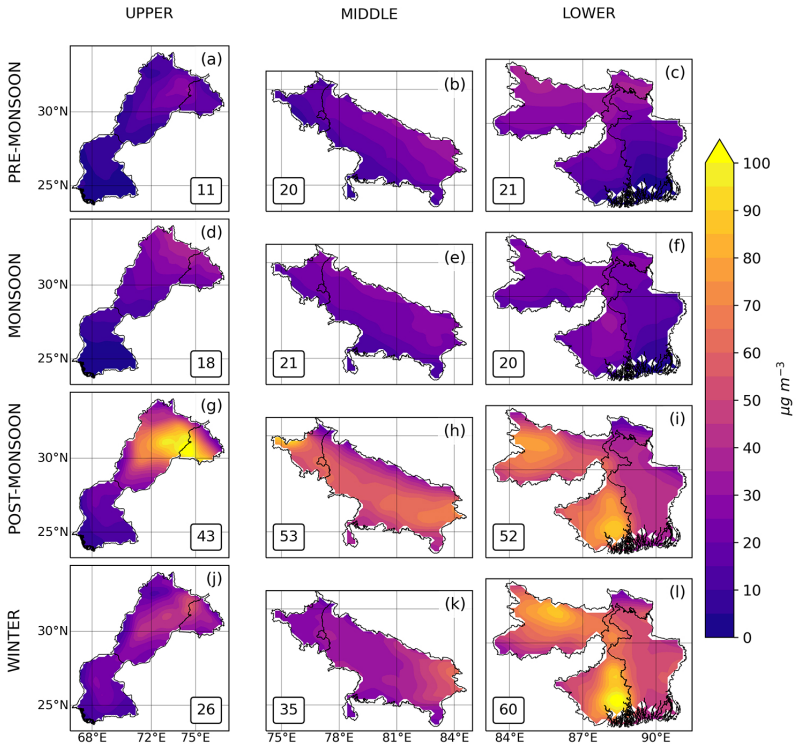

Figure 6. Seasonal mean distributions of total OA over the upper, middle and lower IGP. The numbers inset of pre-monsoon (a–c), monsoon (d–f), post-monsoon (g–i), and winter (l–n) seasons denote the regional mean total OA value.

The sum of primary and secondary OA contributes by mass between 17% and 31% of $PM_{2.5}$ across the IGP, with contributions from POA and SOA varying with season. During the pre-monsoon season, OA contributes 11–21 μg m^{-3} to $PM_{2.5}$, representing 17–22% of the total mass. A similar mass contribution is found during the monsoon season (18–21 μg m^{-3}) but with higher percentage contribution to $PM_{2.5}$ (20–31%). The percentage mass contribution of OA to $PM_{2.5}$ is similar during the post-monsoon (28–31%, 43–52 μg m^{-3}) and winter (22–31%, 26–60 μg m^{-3}), with higher mass contribution during post-monsoon for the middle and lower IGP and during the winter season for the lower IGP. Our results for modeled $PM_{2.5}$ composition confirm the significance of OA contribution to fine particulate matter, and we analyse in more detail OA and its components in the next sections.

3.3 Seasonal Distribution of Surface OA

https://doi.org/10.5194/acp-2021-69
Preprint. Discussion started: 4 February 2021

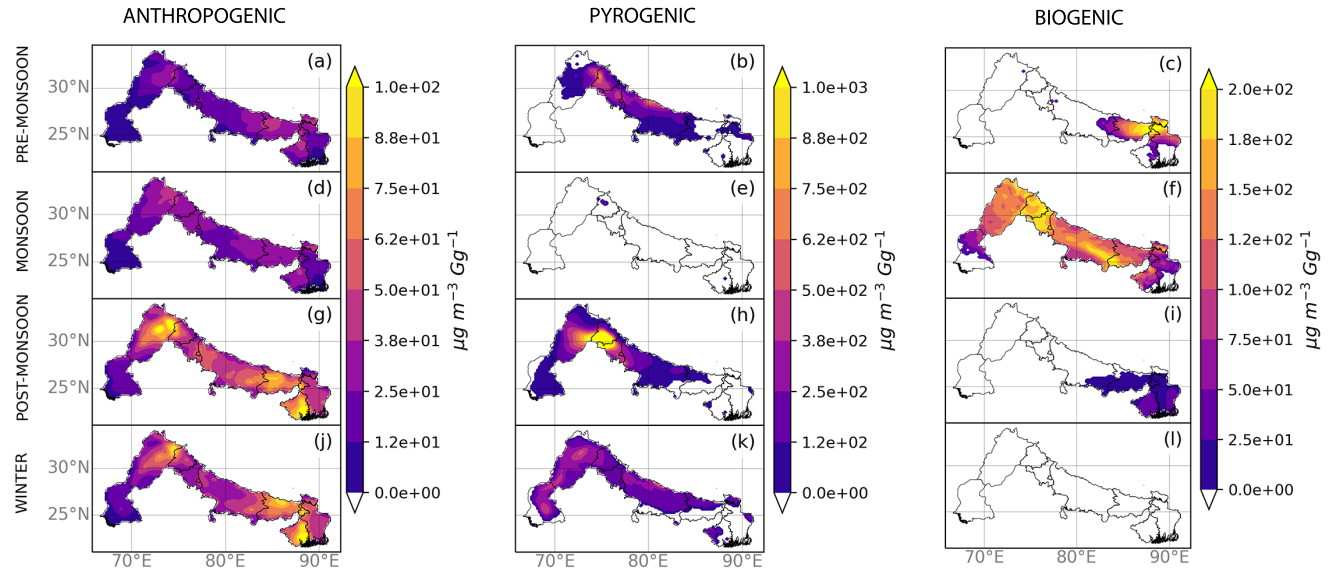

Figure 7. Seasonal sensitivity of total OA to changes in (left column) anthropogenic, (middle column) pyrogenic, and (right column) biogenic emissions (μ g m^{-3}Gg^{-1}). The sensitivity calculation is described in the main text. Regions marked as white shows where sensitivity corresponds to OA concentrations below the set threshold of 1 μg m^{-3}.

Figure 6 shows the season mean distributions of total OA with the corresponding POA and SOA distributions shown by Figures A2 and A3. We generally find that POA dominates seasonal values of total OA across the IGP, with the exception of the post-monsoon season when SOA and POA have comparable values.

During the post-monsoon season (Figure 6g-i), the largest OA concentrations are over the upper IGP at the border of Pakistani and Indian Punjab ($>$ 80 μg m^{-3}), where POA values can exceed 50 μg m^{-3}. Although the largest regional mean is found over the lower IGP (52 μg m^{-3}) due to urban anthropogenic emissions in and around Kolkata and Patna where values are $>$70 μg m^{-3}. Over the middle IGP, the mean OA value is similar to the lower IGP (52 μg m^{-3}) but shows a more homogeneous distribution, with the highest OA values found at the borders between upper and lower IGP. Regional mean POA values range 23–29 μg m^{-3} (Figure A2g-i), similar to SOA values (20–24 μg m^{-3}, Figure A3g-i). POA levels are much higher than SOA over the Punjab states in India and Pakistan and in the Indian lower IGP (40–70 and 30–40 μg m^{-3} for POA and SOA, respectively). Over the middle IGP, SOA is generally higher than POA (29 and 24 μg m^{-3} for SOA and POA, respectively), with highest concentrations of SOA found in the lower Uttar Pradesh (up to 40 μg m^{-3}). Over Bangladesh and the Pakistani state of Sindth POA and SOA have comparable values ($<$35 μg m^{-3}).

We find that during the post-monsoon season, the OA distribution across the IGP is most sensitive to changes in anthropogenic emissions (Figure 7g-i), with the greatest sensitivity of the Indian part of the lower IGP and in the Punjabi Pakistan. We find that OA over the Delhi NCT megacity is not sensitive to these changes unlike other cities mentioned previously, so that Delhi is not one of the main hotspots of OA across IGP during this season (Figure 6h) unlike it is for $PM_{2.5}$ (Figure 3h).

https://doi.org/10.5194/acp-2021-69
Preprint. Discussion started: 4 February 2021


Atmospheric Chemistry and Physics Discussions

We find that the sensitivity of POA and SOA to changes in anthropogenic emissions are comparable over the Punjab states and across major cities (Figures A4g, A5g). The sensitivity of OA to changes in biomass burning is localised with POA most influenced by fires from Indian Punjab (Figure A4h) and corresponding impact on SOA extending over Pakistan and towards the middle IGP (Figure A5h). Similarly, biogenic emissions play only a localised role in OA and SOA concentrations where biogenic emissions are still significant during this season (Figures 7i and A5i).

We find that the largest seasonal mean values of OA are during winter over the lower IGP (60 μg m^{-3}, Figure 6j-l) with contributing localised peaks over Kolkata and Patna (>80 μg m^{-3}) and at the border between Pakistan and India (ranging 40–70 μg m^{-3}). Seasonal mean values of POA and SOA also peak during winter over the lower IGP (34 μg m^{-3} and 26 μg m^{-3}, respectively.) During winter, the OA distribution is shaped by anthopogenic and pyrogenic emissions (Figure 7j-l). POA concentrations are determined mostly by anthropogenic emissions so that the resulting spatial distribution does not change much from the post-monsoon season (Figure A2j). SOA is also mostly determined by anthropogenic emissions but mainly over the lower IGP and localised areas between Pakistan and India (Figure A5j). POA and SOA are also sensitive to pyrogenic emissions, but during this season it is limited to fires over the Indus basin in Pakistan, with additional sensitivity for SOA to fires over the central IGP (Figures A4k, A5k) with sensitivity $<5\times10^2$ μg m^{-3} Gg^{-1}). We find that biogenic emissions do not significantly influence OA during winter.

During pre-monsoon and monsoon seasons, the OA distributions (Figure 6a-f) have similar mean values over the middle and lower IGP (20–21 μg m^{-3}) and lower mean values over the upper IGP (11 and 18 μg m^{-3}, respectively). The highest POA concentrations are found at the border on India and Pakistan and over the lower IGP ($\simeq$30 and 40 μg m^{-3}, respectively). In both seasons, mean SOA concentrations are below 15 μg m^{-3}) across all the IGP. During pre-monsoon and monsoon seasons, OA concentrations are sensitive to anthropogenic emissions across the IGP with similar spatial distributions (Figure 7a,d). Pyrogenic emissions influence the OA distribution during the pre-monsoon season over the central IGP (Figure 7b), but OA is an order of magnitude less sensitive to these emissions compared with the post-monsoon season (Figure 7h). During the monsoon season, the influence of fires on OA is negligible across the IGP. The influence of biogenic emissions on OA, determined exclusively in our model via SOA, is limited to the lower IGP during the pre-monsoon season. During the monsoon season, these emissions have a widespread impact on OA (Figure 7f) with seasonal mean peak sensitivity of up to 2.3×10^2 μg m^{-3} Gg^{-1}.

3.4 Seasonal Distribution of SOA Volatility

We use aerosol volatility to describe how SOA is partitioned between the gas and particle phase to understand when it contributes to $PM_{2.5}$ mass loading. Figure 8 shows the seasonal mean volatility distributions for SOA across the IGP simulated using the 1-D VBS model in WRF-Chem (Knote et al., 2015). Seasonal and regional variations reflect changes in the physical and chemical environment in which the SOA is formed. Broadly, we find a gradual increase in the volatility of SOA from the pre-monsoon season to the winter season, mainly reflecting the increase in the mean OA loading (Figure 6). Higher OA loading leads to a shift in the gas-particle partitioning towards more volatile bins, reflected in the seasonal variation in the population of

https://doi.org/10.5194/acp-2021-69
Preprint. Discussion started: 4 February 2021

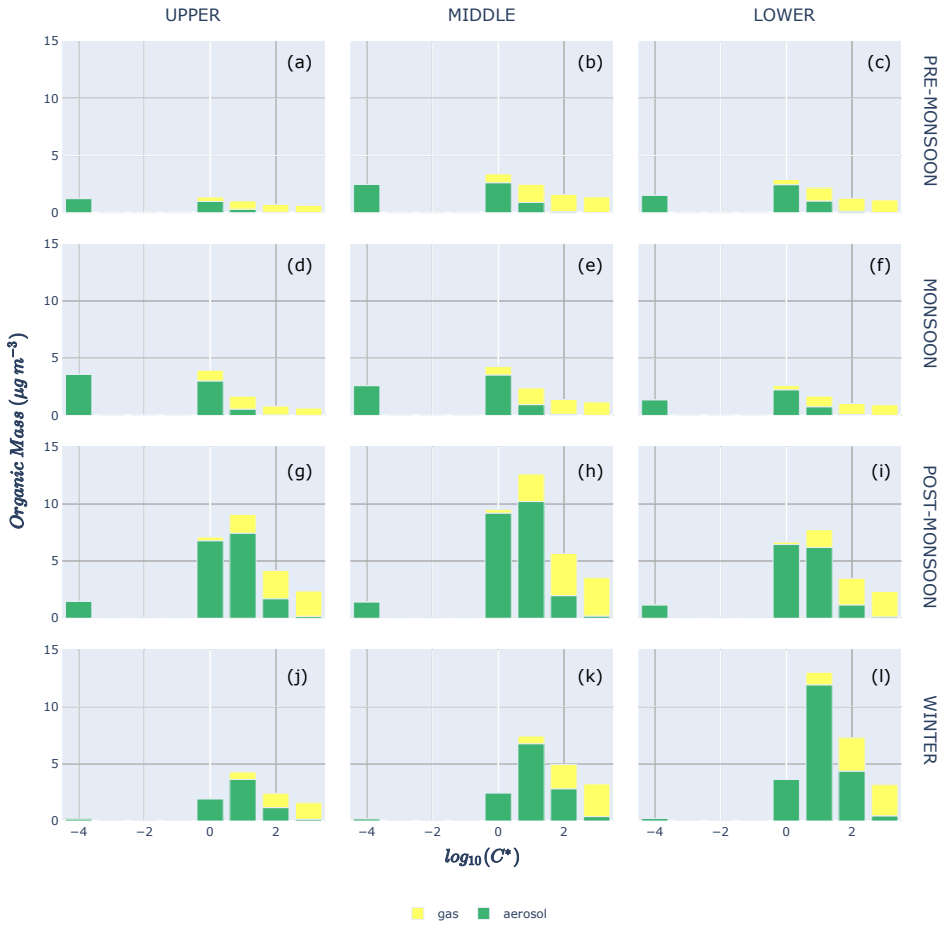

Figure 8. Seasonal mean volatility distribution of SOA over the upper, middle, and lower IGP as calculated within the WRF-Chem 1-D VBS scheme for (a–c) pre-monsoon, (d–f) monsoon, (g–i) post-monsoon, and (j–l) winter seasons.

https://doi.org/10.5194/acp-2021-69
Preprint. Discussion started: 4 February 2021


Atmospheric Chemistry and Physics Discussions

the inert bin (denoted here as $log_{10}C^* = -4$, as described above). The contribution of this inert bin is negligible during winter and peaks during the monsoon season, with intermediate values during the pre-monsoon and post-monsoon transition seasons.

During the post-monsoon season, the particle phase organic mass is present at high volatility bins up to $log_{10}C^* = 2$. The largest particle phase mass loading (10 μg m^{-3}) is found over the middle IGP. The upper and lower IGP show a similar volatility distribution as the middle IGP but with lower mass loadings, with the lower IGP having the lowest mass loadings. The smallest values over the lower IGP reflect the persistence of rainfall over this region that leads to continued removal of water soluble gas-phase and aerosol-phase organics.

Surface-level atmospheric organic mass becomes even more volatile during the winter season, with particle phase organic matter present in all volatility bins. The largest mass loading for SOA are found over the lower IGP (> 10 μg m^{-3}) and decreases westwards towards the upper IGP, reflecting the E-W gradient of the total OA loading (Figure 6j–l).

SOA during the pre-monsoon (Figure 8 a–c) and monsoon (Figure 8 d–f) seasons are characterised by a volatility $\leq log_{10}C^* = 1$, and with aerosol masses lower than 5 μg m^{-3} for each volatility bin in both seasons. The higher volatility bins ($log_{10}C^* = 2$ and $log_{10}C^* = 2$) are occupied exclusively by gas-phase organic compounds. We attribute this to water-soluble SVOCs being washed out by monsoonal rainfall. The washout of SVOCs results in gas-aerosol re-partitioning to establish thermodynamic equilibrium, associated with particle phase organics partitioning to the gas-phase. Aerosols are also removed via wet and dry deposition but we find most of the loss of SVOCs and SOA mass is lost via the gas phase (Knote et al., 2015). This also helps to explain the low levels of OA during the pre-monsoon and monsoon seasons (Figure 6). The OA volatility distribution is similar across the IGP, reflecting an approximately uniform physical environment during the two seasons (Figures A1 and 7).

4 Concluding Remarks

We used the WRF-Chem regional atmospheric chemistry model to understand the influence of anthropogenic, pyrogenic and biogenic emissions and meteorology on seasonal variations of the magnitude, distribution, and composition of $PM_{2.5}$ and organic aerosol across the Indo-Gangetic Plain (IGP) during 2017/2018.

We find that the IGP experiences the highest seasonal mean levels of $PM_{2.5}$ during the post-monsoon (October—December, 166 $\mu g\ m^{-3}$) and winter (January—February, 145 $\mu g\ m^{-3}$) seasons with an heterogeneous distribution, in agreement with previous studies. The magnitude and distribution of anthropogenic emissions across the IGP are approximately constant throughout the year. During the post-monsoon season, agricultural burning emissions of post-harvest residues influence $PM_{2.5}$ mostly over the upper and middle IGP, particularly affecting the Indian and Pakistani Punjab region. These additional emissions are exacerbated by high pressure weather systems that reduce ventilation of surface air pollution to the free troposphere. During the winter season, ongoing anthropogenic emissions, wind patterns, and a seasonally shallow boundary layer result in a gradient in air quality from the upper to lower IGP, with the highest $PM_{2.5}$ values (in excess of 250 $\mu g\ m^{-3}$) over Kolkata and the state of Bihar. During the pre-monsoon (March–May) and monsoon (June–September) seasons wet scavenging of hydrophilic gas-phase aerosol precursors and aerosols, and more rigorous vertical mixing, reduces levels of $PM_{2.5}$ (95-79 $\mu g\ m^{-3}$ re-

https://doi.org/10.5194/acp-2021-69
Preprint. Discussion started: 4 February 2021


Atmospheric Chemistry and Physics Discussions

spectively). We find that during the pre-monsoon seasons the impact of biomass-burning over the central IGP is an order of magnitude less that during the post-monsoon season. Generally, we find that $PM_{2.5}$ composition has a stronger seasonal variation than a geographical variation within each season. Total inorganic species dominate $PM_{2.5}$ composition (30-80%), with water uptake contributing substantially to the $PM_{2.5}$ mass especially over the lower IGP (up to 40%).

We find that OA represents a significant contribution to $PM_{2.5}$ throughout the year. On an annual mean basis, OA represents 17–30% of $PM_{2.5}$, with higher contributions during post-monsoon and winter seasons. Typically, POA contributes more to the OA loading than SOA in all seasons across the IGP. Anthropogenic and pyrogenic sources impact POA and SOA with similar patterns of $PM_{2.5}$ across the IGP during all seasons. Biogenic sources have a significant impact on SOA distribution across the IGP during the monsoon season but are limited to the lower IGP during the pre- and post- monsoon seasons. We find that the volatility distribution of SOA is driven mainly by the mean total OA loading and the washout of aerosols and gas-phase aerosol precursors that result in SOA being less volatile during the pre-monsoon and monsoon season than during the post-monsoon and winter seasons.

Mitigating levels of $PM_{2.5}$ over the IGP will require a range of regional and state-level policies that address the influences of intra- and inter- state anthropogenic, pyrogenic, and biogenic emissions. The relative influence of these emissions on $PM_{2.5}$ and the broader photochemical environment will likely change in the context of a warmer climate, e.g. biogenic emissions will increase as they are temperature dependent. It is therefore imperative that future studies should also consider sub-regional and city spatial scales, where individual sectors will be more important, and where there is the highest population density that will suffer from poor air quality.

https://doi.org/10.5194/acp-2021-69
Preprint. Discussion started: 4 February 2021

Atmospheric Chemistry and Physics Discussions

Appendix A: Meteorological drivers, POA and SOA distribution

Figure A1 shows the mean seasonal WRF-Chem meteorological driver or pre-monsoon, monsoon and post-monsoon 2017 and winter 2018. Figure A2, to A5 show POA and SOA distribution over the IGP and their sensitivity to emissions drivers.

https://doi.org/10.5194/acp-2021-69
Preprint. Discussion started: 4 February 2021

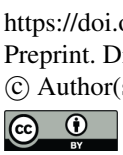

Atmospheric Chemistry and Physics Discussions

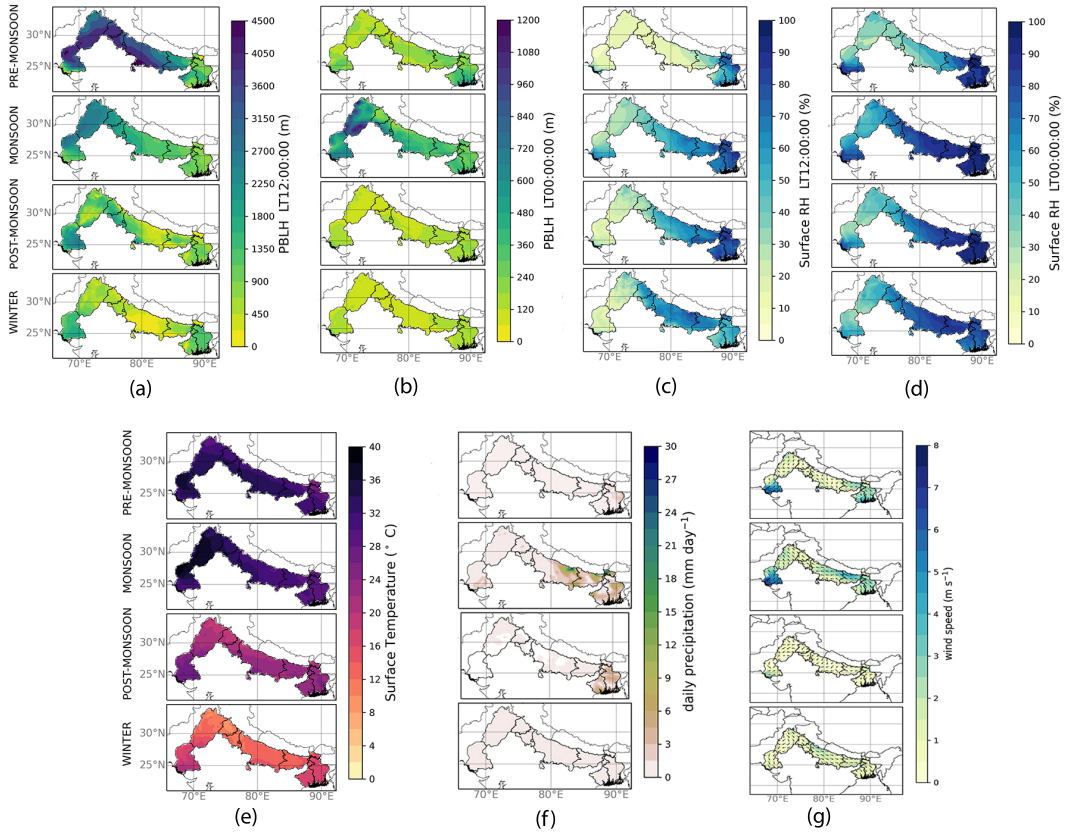

Figure A1. Seasonal mean WRF-Chem meteorological fields: (a) daytime planetary boundary layer height (m); (b) nighttime planetary boundary layer height (m); (c) daytime surface relative humidity (%); (d) nighttime surface relative humidity (%); (e) surface temperature at 2 m (°C; (f) daily precipitation rate (mm day^{-1})); and (g) wind speed (m s^{-1}) and direction at 10 m.

https://doi.org/10.5194/acp-2021-69
Preprint. Discussion started: 4 February 2021

Atmospheric Chemistry and Physics Discussions

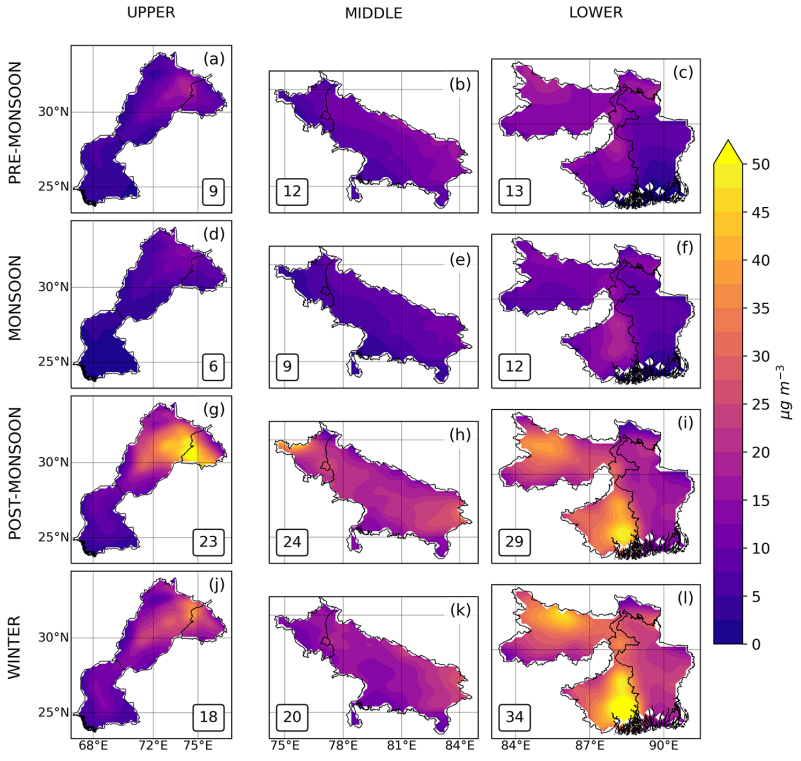

Figure A2. Seasonal mean distributions of POA over the upper, middle and lower IGP. The numbers inset of pre-monsoon (a–c), monsoon (d–f), post-monsoon g–i), and winter (j–l) seasons denote the regional mean POA value.

https://doi.org/10.5194/acp-2021-69
Preprint. Discussion started: 4 February 2021

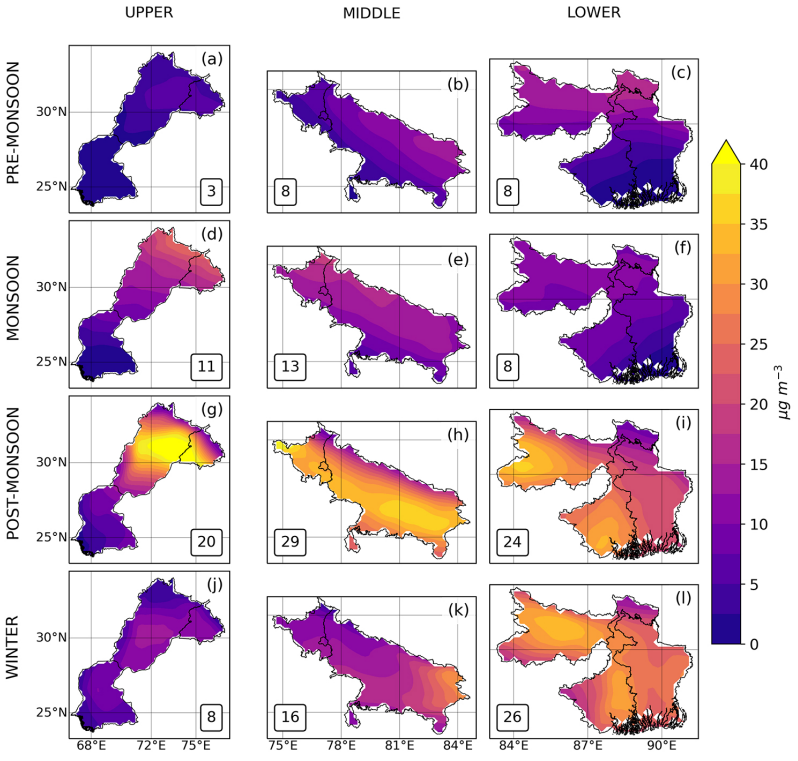

Figure A3. As A2 but for SOA.

https://doi.org/10.5194/acp-2021-69
Preprint. Discussion started: 4 February 2021

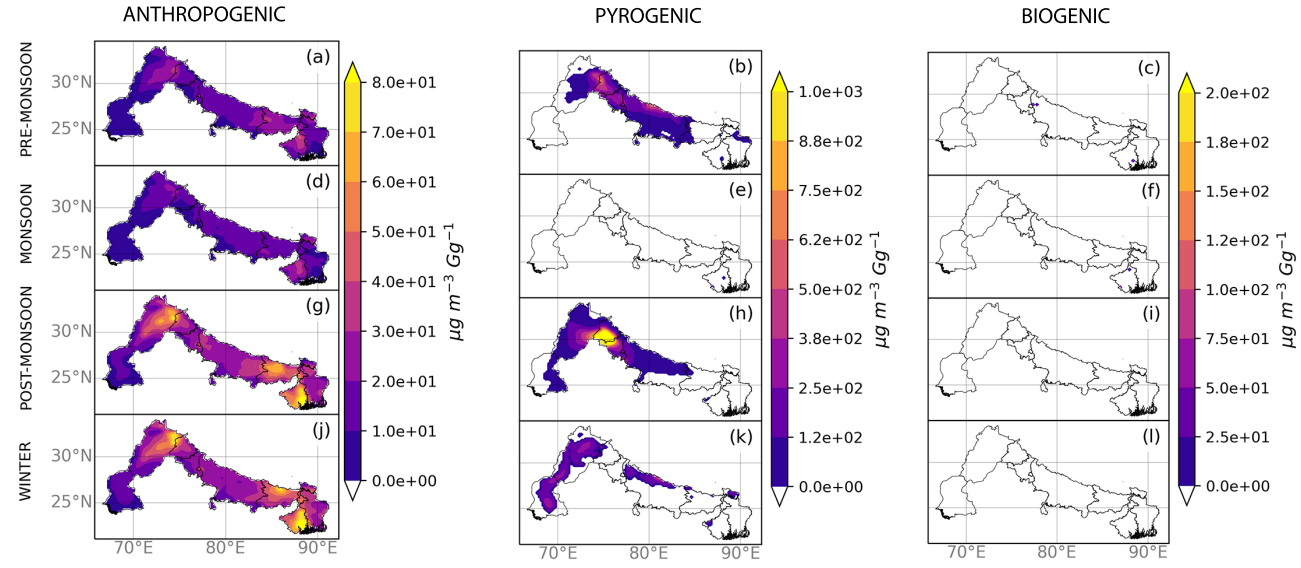

Figure A4. Seasonal sensitivity of POA to changes in (left column) anthropogenic, (middle column) pyrogenic, and (right column) biogenic emissions (μ g m^{-3}Gg^{-1}). The sensitivity calculation is described in the main text. Regions marked as white shows where sensitivity corresponds to OA concentrations below the set threshold of 1 μg m^{-3}.

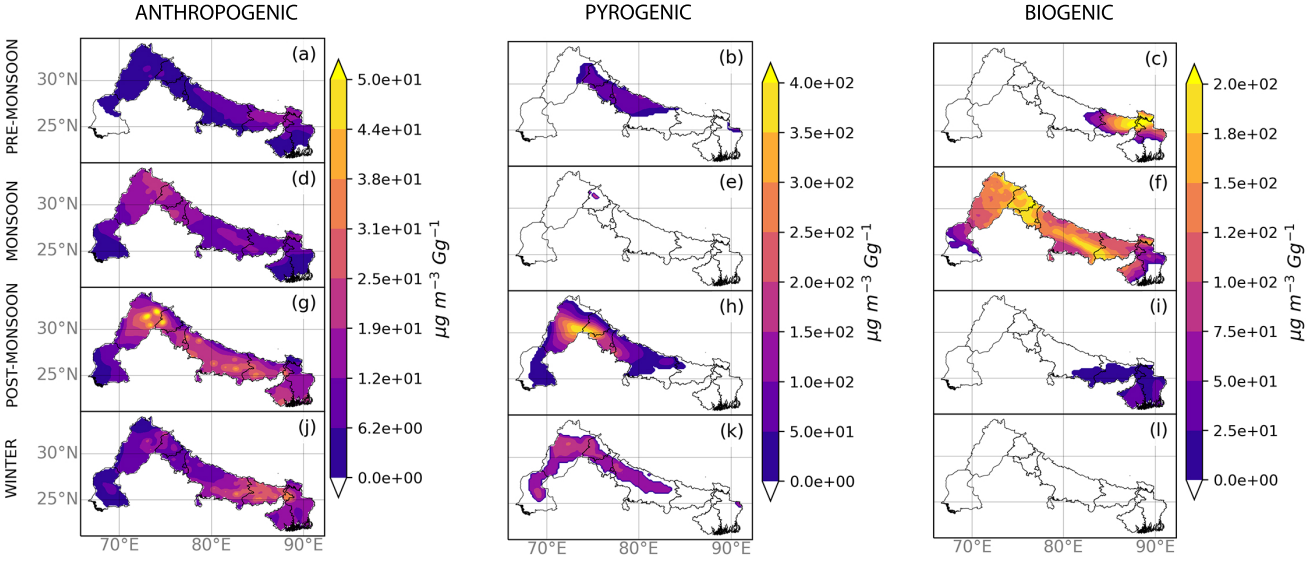

Figure A5. As Figure A4 but for SOA.

https://doi.org/10.5194/acp-2021-69
Preprint. Discussion started: 4 February 2021


Atmospheric Chemistry and Physics Discussions

Appendix B: WRF-Chem set-up and evaluation

Table A1 summarises the parametrisation for meteorology we use in WRF-Chem. The following subsections describe the evaluation of model result with ground based observation, OA values from literature and with satellite AOD respectively.

Ground-based Measurements evaluation

We use ground-based measurements from the Central Pollution Control Board and the U.S. Embassies, which are available for our 2017/2018 study period, and accessed through the OpenAQ Platform (OpenAQ). Data from Pakistan are only available from 2019 so we use 2019 data for the monsoon and post-monsoon seasons and data from 2020 for the winter and pre-monsoon seasons.

We apply a cleaning procedure of data for each pollutant. The cleaning procedure followed five sequential steps: 1) Exclude non valid, negative and zero values; 2) exclude hourly data with $z_{score} \geq 3$ respect to daily mean; 3) exclude days with fewer then 12 hourly measurements per day; 4) exclude stations with less then 15 days measurements per simulated season; and 5) exclude all stations but one if there are multiple stations in the same model grid-cell (for statistical independence in the comparison). From this cleaning procedure we get 31 independent stations (Table A2) with a total of seasonal measurements: 63 for CO, 54 for SO_2, 61 for NO_2, 50 for O_3, 84 for $PM_{2.5}$, 20 for PM_{10}. For particulate matter, we compare the dry mass of $PM_{2.5}$ and PM_{10}.

To compare the model against these measurements, we sample the model at the time and location of each measurement. In practice, we identify the model value closest to the measurement. We report seasonal mean statistics.

We evaluate the model using five metrics: the Mean Bias (MB), Root Mean Square Error (RMSE), Normalised Mean Bias (NMB), Mean Normalised Absolute Error (MNAE), and sample Pearson correlation coefficient (r). These metrics are widely used for air quality model evaluation (Zhang et al., 2006; Kumar et al., 2012; Brasseur and Jacob, 2017; Conibear et al., 2018). Table A3 summarises the seasonal mean evaluation of the model with the metrics described.

Organic Aerosols

In the absence of continuous monitoring data of OA, we compare our model OC values with values found in the literature. Table A4 shows the comparison of modeled OC with measurements studies. OA are converted from organic aerosol mass to organic carbon mass assuming OA/OC ratios 1.4 for POA and 2.0 for SOA, following (Knote et al., 2015).

Total AOD column

We compare our modeled prediction against satellite AOD retrievals at 550 nm with a 10 km horizontal resolution obtained from both Terra (MOD04_L2) and Aqua (MYD04_L2) MODIS instruments. We use the best-quality AOD retrievals merged from the dark target and the deep blue algorithms (Levy et al., 2013). We re-grid the 10 km Terra and Aqua MODIS AOD data to the coarse WRF-Chem 20 km$\times$20 km model grid.

https://doi.org/10.5194/acp-2021-69
Preprint. Discussion started: 4 February 2021


Atmospheric Chemistry and Physics Discussions

We calculate the 550 nm AOD using WRF-Chem values at 300 nm and 1000 nm by interpolation using the Ångström power law. We sample the model at the local overpass time of Terra (1030) and Aqua (1330) where there exists at least one best-quality AOD retrieval. We then mean model and MODIS AOD values over time to generate seasonal statistics. Table A5 reports the main statistical metrics for AOD evaluation together with the range of observed and modeled AOD.

https://doi.org/10.5194/acp-2021-69
Preprint. Discussion started: 4 February 2021

Atmospheric Chemistry and Physics Discussions

Table A1. Chosen parametrisations for meteorological processes in WRF-Chem.

Process	**Parametrisation**
Cloud microphysics	Morrison double-moment scheme (Morrison et al., 2005)
Planetary boundary layer	Mellor-Yamada Nakanishi and Niino 2.5 (MYNN2) (Nakanishi and Niino, 2006)
Convection	Grell 3D scheme (Grell and Dévényi, 2002).
Short and long wave radiation	The Rapid Radiative Transfer Model (RRTM) (Iacono et al., 2008).
Land surface	Noah Land Surface Model coupled with a urban canopy model (Ek et al., 2003; Kusaka and Kimura, 2004)

https://doi.org/10.5194/acp-2021-69
Preprint. Discussion started: 4 February 2021


Atmospheric Chemistry and Physics Discussions
Open Access
EGU

Table A2. List of selected ground-based stations and their measurements used for model evaluation.

number	city	station name	latitude	longitude
1	Agra	Sanjay Palace	27.20	78.01
2	Delhi	Income Tax Office	28.62	77.25
3	Delhi	Delhi Technological University	28.74	77.12
4	Delhi	Shadipur	28.65	77.16
5	Delhi	Anand Vihar	28.65	77.32
6	Delhi	Punjabi Bagh	28.67	77.12
7	Delhi	NSIT Dwarka	28.59	77.05
8	Delhi	IHBAS	28.68	77.31
9	Delhi	Mandir Marg	28.63	77.20
10	Delhi	R K Puram	28.56	77.17
11	Dhaka	US Diplomatic Post: Dhaka	23.80	90.42
12	Faridabad	Sector16A Faridabad	28.41	77.31
13	Gaya	Collectorate - Gaya - BSPCB	24.75	84.94
14	Gurgaon	Vikas Sadan Gurgaon - HSPCB	28.45	77.03
15	Haldia	Haldia - WBPCB	22.06	88.11
16	Islamabad	US Diplomatic Post: Islamabad	33.72	73.12
17	Jaipur	VK Industrial Area Jaipur - RSPCB	26.97	75.77
18	Jodhpur	Collectorate Jodhpur - RSPCB	26.29	73.04
19	Kanpur	Nehru Nagar	26.47	80.33
20	Karachi	US Diplomatic Post: Karachi	24.84	67.01
21	Kolkata	US Diplomatic Post: Kolkata	22.56	88.36
22	Kolkata	Rabindra Bharati University, Kolkata - WBSPCB	22.63	88.38
23	Lahore	US Diplomatic Post:Lahore	31.56	74.34
24	Lucknow	Central School	26.85	81.00
25	Lucknow	Lalbagh, DN Park	26.85	80.94
26	Muzaffarpur	Collectorate - Muzaffarpur - BSPCB	26.08	85.41
27	Panchkula	Sector 6 Panchkula - HSPCB	30.71	76.85
28	Patna	IGSC Planetarium Complex - Patna - BSPCB	25.36	85.08
29	Peshawar	US Diplomatic Post: Peshawar	34.01	71.54
30	Rohtak	MD University, Rohtak - HSPCB	28.88	76.62
31	Varanasi	Ardhali Bazar	25.35	82.98

https://doi.org/10.5194/acp-2021-69
Preprint. Discussion started: 4 February 2021

Atmospheric Chemistry and Physics Discussions

Table A3. Statistical evaluation of model performance with ground based measurements for main PM and main gas pollutants.

pollutant	**season**	**NMB**	**NMAE**	**MB [$\mu g\ m^{-3}$]**	**RMSE [$\mu g\ m^{-3}$]**	**r**
$PM_{2.5}$	pre-monsoon	0.12	0.31	10	34	0.62
	monsoon	0.41	0.65	19	36	0.09
	post-monsoon	0.19	0.28	33	62	0.84
	winter	0.004	0.28	0.7	53	0.69
PM_{10}	pre-monsoon	0.15	0.59	32	133	0.11
	monsoon	-0.21	0.28	-25	46	0.69
	post-monsoon	-0.14	0.36	-41	122	0.66
	winter	-0.25	0.43	-64	131	-0.85
CO	pre-monsoon.	-0.64	0.64	-643	825	0.44
	monsoon	-0.55	0.55	-428	567	0.12
	post-monsoon	-0.65	0.65	-1439	2272	0.29
	winter	-0.52	0.61	-703	1163	-0.20
NO_2	pre-monsoon	0.14	0.95	6	57	0.27
	monsoon	0.46	1.00	11	32	0.08
	post-monsoon	0.65	1.44	36	97	0.15
	winter	0.31	0.98	17	66	0.30
O_3	pre-monsoon	1.59	1.67	75	91	-0.52
	monsoon	2.92	2.92	64	66	-0.12
	post-monsoon	2.96	2.98	98	113	-0.75
	winter	2.87	2.92	71	87	-0.55
SO_2	pre-monsoon	0.25	0.85	3	13	0.04
	monsoon	0.27	1.38	4	34	-0.18
	post-monsoon	2.36	2.44	33	49	0.51
	winter	1.85	2.15	27	43	0.04

https://doi.org/10.5194/acp-2021-69
Preprint. Discussion started: 4 February 2021

Atmospheric Chemistry and Physics Discussions

Table A4. Comparison of modeled OC with measurements studies in the literature. Model values refers to the mean over the corresponding season of observations.

location	period	species	OC measurements [$\mu g\ m^{-3}$]	OC model [$\mu g\ m^{-3}$]	reference
Delhi	Jan-Feb 13-16	$PM_{2.5}$	23.6 ± 12.9	23.4	Jain et al. (2020)
	Mar-May 13-16		9.82 ± 4.16	13.3	
	Jun-Set 13-16		6.77 ±2.63	12.1	
	Oct-Dec 13-16		25.2 ±14.7	38.6	
Delhi	Jan-Feb 13-16	PM_{10}	30.1±12.1	23.5	Jain et al. (2020)
	Mar-May 13-16		23.4 ± 10.7	13.4	
	Jun-Set 13-16		15.9 ±9.7	12.3	
	Oct-Dec 13-16		39.4 ±15.6	38.7	
Kanpur	Oct-Nov 08	.	53.3 ±21.2	37.2	Ram et al. (2012)
	Dec 08 - Feb 09	PM_{10}	29 ± 14.5	21.9	
	Mar-Apr 09		23.1 ± 11.5	12.3	
Kharagpur	Nov 09 - Mar 10	$PM_{2.5}$	30.7± 12.1	42.0	Srinivas and Sarin (2014)
Kolkata	Jan-06	$PM_{2.5}$	18.5±2.0	67.2	Chatterjee et al. (2012)
	Apr-May 06		15.5± 3.6	7.8	
	Jul-06		5±1	14.3	
	Oct-Nov 06		11.5±5.0	57.4.	
Lahore	Jan-07	$PM_{2.5}$	76.5	34.0	Stone et al. (2010)
	Apr-May-07		43.5	20.0	
	Jul-07		31.5	18.2	
	Oct-Nov 07		111.2	61.0	

https://doi.org/10.5194/acp-2021-69
Preprint. Discussion started: 4 February 2021

Atmospheric Chemistry and Physics Discussions

Table A5. Seasonal comparison of modeled total AOD column and satellite AOD observations for the Terra and Aqua instruments over the IGP.

satellite	season	MB	NMB	NMAE	RMSE	r	range obs	range model
Terra	pre-monsoon	0.33	0.53	0.56	0.44.	0.53	0.06 - 1.78	0.10 - 2.29
	monsoon	0.04	0.05	0.45	0.52	0.35	0.00 - 3.42	0.10 - 3.78
	post-monsoon	-0.05	-0.06	0.25	0.25	0.76	0.07 - 3.50	0.12 - 1.71
	winter	-0.11	-0.19	0.30	0.21	0.64	0.05 - 1.74	0.11 - 1.16
Aqua	pre-monsoon	0.27	0.44	0.49	0.40	0.52	0.07 - 3.50	0.08 - 2.82
	monsoon	-0.18	-0.19	0.43	0.53.	0.35	0.04 - 2.53	0.11 - 3.17
	post-monsoon	-0.05	-0.06	0.25	0.23	0.74	0.06 - 2.23	0.12 - 1.47
	winter	-0.08	-0.14	0.33	0.22	0.47	0.09 - 1.17	0.08 - 1.2

https://doi.org/10.5194/acp-2021-69
Preprint. Discussion started: 4 February 2021

Atmospheric Chemistry and Physics Discussions

Code and data availability. All the data and materials used in this study are freely available. The WRF-Chem model code is available from https://www2.acom.ucar.edu/wrf-chem. NCEP FNL global tropospheric analyses were taken from https://rda.ucar.edu/datasets/ds083.3/. CAM-CHEM global model results were downloaded from https://www.acom.ucar.edu/cam-chem/cam-chem.shtml. The EDGAR-HTAPv2.2 emissions dataset ready for be used in WRF-Chem were downloaded from https://www2.acom.ucar.edu/wrf-chem/wrf-chem-tools-community. The FINN biomass burning emissions dataset was downloaded from https://bai.acom.ucar.edu/Data/fire/. Ground based observation used for the model evaluation where obtained from https://openaq.org/. The MODIS data are available from https://ladsweb.modaps.eosdis.nasa.gov/. Metadata that describe our calculations are available from https://github.com/catemgn/aqIGP; we move the metadata to zenodo once the paper has been accepted for publication.

Author contributions. CM and PIP conceived the study and methodology. CM set-up the model with support from CK. CM performed the simulations, and led the model evaluation and data analysis, and interpreted the results together with PIP, CK and TJW. FY provided the AOD observations to be compared with the model AOD. CM and PIP wrote the paper, with input from all co-authors.

Competing interests. The authors declare that they have no conflict of interest.

Acknowledgements. CM is supported by funding from the Ford Motor Company University Research Program (#2016-2007R). The work of Fei Yao was supported by the China Scholarships Council/University of Edinburgh Scholarships. This study was funded as part of NERC's support of the National Centre for Earth Observation: PIP was supported by grant number #NE/R016518/1. We thank Jim Anderson, Wei Shen, and Sandy Winkler for helpful discussions. CM is thankful to the WRF-Chem community for the support received, in particular to S. Walters, G. Pfister, M. Barth, for providing support in the WRF-Chem online forum, and to L. Conibear, D. Lowe, R. Kumar, S. Archer-Nicholls, M. Morichetti for discussion and clarifications on specific technical issues. We acknowledge the use of the WRF-Chem preprocessor tool (anthro-emiss, fire-emiss, bioemiss, mozbc) provided by the Atmospheric Chemistry Observations and Modeling Lab (ACOM) of NCAR. We also acknowledge the use of the following software and packages for the post-processing and analysis of WRF-Chem simulations: ArcGIS 10.7, Python 3.6, xarray (Hoyer and Hamman, 2017), pandas (The pandas dev. Team, 2020) numPy (Harris et al., 2020) cartopy (Met Office, 2010 - 2015), plotly (Plotly Technologies Inc., 2015), matplotlib (Hunter, 2007), salem (Maussion et al., 2017). Administrative areas for IGP were taken from GADM (https://gadm.org).

https://doi.org/10.5194/acp-2021-69
Preprint. Discussion started: 4 February 2021

Atmospheric Chemistry and Physics Discussions

References

ACOM-NCAR: WRF-Chem Tools for the Community, https://www2.acom.ucar.edu/wrf-chem/wrf-chem-tools-community, last access: 30 November 2020.

Agarwala, M. and Chandel, A.: Temporal role of crop residue burning (CRB) in Delhi's air pollution, Environ. Res. Lett., 15, 114 020, https://doi.org/https://doi.org/10.1088/1748-9326/abb854, 2020.

Ahmadov, R., McKeen, S., Robinson, A., Bahreini, R., Middlebrook, A., De Gouw, J., Meagher, J., Hsie, E.-Y., Edgerton, E., Shaw, S., et al.: A volatility basis set model for summertime secondary organic aerosols over the eastern United States in 2006, J. Geophys. Res.-Atmos., 117, https://doi.org/https://doi.org/10.1029/2011JD016831, 2012.

Ahmed, T., Ahmad, B., and Ahmad, W.: Why do farmers burn rice residue? Examining farmers' choices in Punjab, Pakistan, Land Use Policy, 47, 448–458, https://doi.org/https://doi.org/10.1016/j.landusepol.2015.05.004, 2015.

Alam, K., Mukhtar, A., Shahid, I., Blaschke, T., Majid, H., Rahman, S., Khan, R., Rahman, N., et al.: Source apportionment and characterization of particulate matter (PM_{10}) in urban environment of Lahore, Aerosol Air Qual. Res., 14, 1851–1861, https://doi.org/https://doi.org/10.4209/aaqr.2014.01.0005, 2014.

Begum, B. A., Hopke, P. K., and Markwitz, A.: Air pollution by fine particulate matter in Bangladesh, Atmos. Pollut. Res., 4, 75–86, https://doi.org/https://doi.org/10.5094/APR.2013.008, 2013.

Behera, S. N. and Sharma, M.: Spatial and seasonal variations of atmospheric particulate carbon fractions and identification of secondary sources at urban sites in North India, sharma2016spatio, 22, 13 464–13 476, https://doi.org/https://doi.org/10.1007/s11356-015-4603-7, 2015.

Bergström, R., Denier Van Der Gon, H., Prévôt, A. S., Yttri, K. E., and Simpson, D.: Modelling of organic aerosols over Europe (2002–2007) using a volatility basis set (VBS) framework: application of different assumptions regarding the formation of secondary organic aerosol, Atmos. Chem. Phys., 12, 8499–8527, 2012.

Bhowmik, H. S., Naresh, S., Bhattu, D., Rastogi, N., Prévôt, A. S., and Tripathi, S. N.: Temporal and spatial variability of carbonaceous species (EC; OC; WSOC and SOA) in $PM_{2.5}$ aerosol over five sites of Indo-Gangetic Plain, Atmos. Pollut. Res., https://doi.org/https://doi.org/10.1016/j.apr.2020.09.019, 2020.

Bran, S. H. and Srivastava, R.: Investigation of $PM_{2.5}$ mass concentration over India using a regional climate model, Environ. Pollut., 224, 484–493, https://doi.org/https://doi.org/10.1016/j.envpol.2017.02.030, 2017.

Brasseur, G. P. and Jacob, D. J.: Modeling of atmospheric chemistry, Cambridge University Press, 2017.

Buchholz, R. R., Emmons, L. K., and Tilmes, S. a.: CESM2.1/CAM-chem Instantaneous Output for Boundary Conditions, https://doi.org/10.5065/NMP7-EP60, subset: Lat: 0 to 50, Lon: 50 to 100, October 2017 - February 2018, Accessed 29 March 2020, 2019.

Chatterjee, A., Dutta, C., Jana, T., and Sen, S.: Fine mode aerosol chemistry over a tropical urban atmosphere: characterization of ionic and carbonaceous species, J. Atmos. Chem., 69, 83–100, https://doi.org/https://doi.org/10.1007/s10874-012-9231-8, 2012.

Chauhan, B. S., Mahajan, G., Sardana, V., Timsina, J., and Jat, M. L.: Productivity and sustainability of the rice–wheat cropping system in the Indo-Gangetic Plains of the Indian subcontinent: problems, opportunities, and strategies, in: Adv. Agron., vol. 117, pp. 315–369, Elsevier, https://doi.org/https://doi.org/10.1016/B978-0-12-394278-4.00006-4, 2012.

https://doi.org/10.5194/acp-2021-69
Preprint. Discussion started: 4 February 2021

Chowdhury, Z., Zheng, M., Schauer, J. J., Sheesley, R. J., Salmon, L. G., Cass, G. R., and Russell, A. G.: Speciation of ambient fine organic carbon particles and source apportionment of $PM_{2.5}$ in Indian cities, J. Geophys. Res.-Atmos., 112, https://doi.org/https://doi.org/10.1029/2007JD008386, 2007.

Chuang, W. K. and Donahue, N. M.: A two-dimensional volatility basis set–Part 3: Prognostic modeling and NOx dependence, Atmos. Chem. Phys., 16, 123–134, https://doi.org/https://doi.org/10.5194/acp-16-123-2016, 2016.

Conibear, L., Butt, E. W., Knote, C., Arnold, S. R., and Spracklen, D. V.: Residential energy use emissions dominate health impacts from exposure to ambient particulate matter in India, Nat. Commun., 9, 1–9, https://doi.org/https://doi.org/10.1038/s41467-018-02986-7, 2018.

Conibear, L. A., Butt, E. W., Knote, C., Lam, N. L., Arnold, S., Tibrewal, K., Venkataraman, C., Spracklen, D. V., and Bond, T. C.: A complete transition to clean household energy can save one–quarter of the healthy life lost to particulate matter pollution exposure in India, Environ. Res. Lett., https://doi.org/https://doi.org/10.1088/1748-9326/ab8e8a, 2020.

CPCB: Air Quality Automatic Monitoring Data, https://app.cpcbccr.com/ccr/#/caaqm-dashboard-all/caaqm-landing, last access: 30 November 2020.

David, L. M., Ravishankara, A., Kodros, J. K., Pierce, J. R., Venkataraman, C., and Sadavarte, P.: Premature mortality due to $PM_{2.5}$ over India: Effect of atmospheric transport and anthropogenic emissions, GeoHealth, 3, 2–10, https://doi.org/https://doi.org/10.1029/2018GH000169, 2019.

DESA, U.: 2018 Revision of World Urbanization Prospects, Tech. rep., United Nation Department of Economic and Social Affairs, 2018.

Donahue, N., Robinson, A., Stanier, C., and Pandis, S.: Coupled partitioning, dilution, and chemical aging of semivolatile organics, Environ. Sci. Technol., 40, 2635–2643, https://doi.org/https://doi.org/10.1021/es052297c, 2006.

Donahue, N. M., Kroll, J., Pandis, S. N., and Robinson, A. L.: A two-dimensional volatility basis set–Part 2: Diagnostics of organic-aerosol evolution, Atmos. Chem. Phys., 12, 615–634, https://doi.org/https://doi.org/10.5194/acp-12-615-2012, 2012.

Ek, M., Mitchell, K., Lin, Y., Rogers, E., Grunmann, P., Koren, V., Gayno, G., and Tarpley, J.: Implementation of Noah land surface model advances in the National Centers for Environmental Prediction operational mesoscale Eta model, J. Geophys. Res.-Atmos., 108, https://doi.org/https://doi.org/10.1029/2002JD003296, 2003.

Emmons, L. K., Walters, S., Hess, P. G., Lamarque, J.-F., Pfister, G. G., Fillmore, D., Granier, C., Guenther, A., Kinnison, D., Laepple, T., et al.: Description and evaluation of the Model for Ozone and Related chemical Tracers, version 4 (MOZART-4), Geosci. Model Dev., 3, 43–67, https://doi.org/https://doi.org/10.5194/gmd-3-43-2010, 2010.

Gani, S., Bhandari, S., Seraj, S., Wang, D. S., Patel, K., Soni, P., Arub, Z., Habib, G., Hildebrandt Ruiz, L., and Apte, J. S.: Submicron aerosol composition in the world's most polluted megacity: the Delhi Aerosol Supersite study., Atmos. Chem. Phys., 19, https://doi.org/https://doi.org/10.5194/acp-19-6843-2019, 2019.

Ghude, S. D., Chate, D., Jena, C., Beig, G., Kumar, R., Barth, M., Pfister, G., Fadnavis, S., and Pithani, P.: Premature mortality in India due to $PM_{2.5}$ and ozone exposure, Geophys. Res. Lett., 43, 4650–4658, https://doi.org/https://doi.org/10.1002/2016GL068949, 2016.

Greenstone, M., , and Fan, C.: Air Quality Life Index, Annual Update, Tech. rep., Energy Policy Institute at The University of Chicago (EPIC), 2020.

Grell, G. A. and Dévényi, D.: A generalized approach to parameterizing convection combining ensemble and data assimilation techniques, Geophys. Res. Lett., 29, 38–1, https://doi.org/https://doi.org/10.1029/2002GL015311, 2002.

Grell, G. A., Peckham, S. E., Schmitz, R., McKeen, S. A., Frost, G., Skamarock, W. C., and Eder, B.: Fully coupled "online" chemistry within the WRF model, Atmos. Enviro., 39, 6957–6975, https://doi.org/https://doi.org/10.1016/j.atmosenv.2005.04.027, 2005.

https://doi.org/10.5194/acp-2021-69
Preprint. Discussion started: 4 February 2021

Atmospheric Chemistry and Physics Discussions

Guenther, A., Karl, T., Harley, P., Wiedinmyer, C., Palmer, P., and Geron, C.: Estimates of global terrestrial isoprene emissions using MEGAN (Model of Emissions of Gases and Aerosols from Nature), Atmos. Chem. and Phys., 6, 3181–3210, https://doi.org/https://doi.org/10.5194/acp-6-3181-2006, 2006.

Gumma, M. K., Thenkabail, P. S., Teluguntla, P., and Whitbread, A. M.: Indo-Ganges River Basin Land Use/Land Cover (LULC) and Irrigated Area Mapping, in: Indus River Basin, pp. 203–228, Elsevier, https://doi.org/https://doi.org/10.1016/B978-0-12-812782-7.00010-2, 2019.

Guttikunda, S. K. and Gurjar, B. R.: Role of meteorology in seasonality of air pollution in megacity Delhi, India, Environ. Monit. Assess., 184, 3199–3211, https://doi.org/https://doi.org/10.1007/s10661-011-2182-8, 2012.

Guttikunda, S. K. and Jawahar, P.: Atmospheric emissions and pollution from the coal-fired thermal power plants in India, Atmos. Environ., 92, 449–460, https://doi.org/https://doi.org/10.1016/j.atmosenv.2014.04.057, 2014.

Guttikunda, S. K., Goel, R., and Pant, P.: Nature of air pollution, emission sources, and management in the Indian cities, Atmos. Environ., 95, 501–510, https://doi.org/https://doi.org/10.1016/j.atmosenv.2014.07.006, 2014.

Hardacre, C. J., Palmer, P. I., Baumanns, K., Rounsevell, M., and Murray-Rust, D.: Probabilistic estimation of future emissions of isoprene and surface oxidant chemistry associated with land-use change in response to growing food needs, Atmospheric Chemistry and Physics, 13, 5451–5472, https://doi.org/10.5194/acp-13-5451-2013, https://acp.copernicus.org/articles/13/5451/2013/, 2013.

Harris, C. R., Millman, K. J., van der Walt, S. J., Gommers, R., Virtanen, P., Cournapeau, D., Wieser, E., Taylor, J., Berg, S., Smith, N. J., Kern, R., Picus, M., Hoyer, S., van Kerkwijk, M. H., Brett, M., Haldane, A., del R'ıo, J. F., Wiebe, M., Peterson, P., G'erard-Marchant, P., Sheppard, K., Reddy, T., Weckesser, W., Abbasi, H., Gohlke, C., and Oliphant, T. E.: Array programming with NumPy, Nature, 585, 357–362, https://doi.org/10.1038/s41586-020-2649-2, https://doi.org/10.1038/s41586-020-2649-2, 2020.

Hoyer, S. and Hamman, J.: xarray: N-D labeled arrays and datasets in Python, Journal of Open Research Software, 5, https://doi.org/10.5334/jors.148, http://doi.org/10.5334/jors.148, 2017.

Hunter, J. D.: Matplotlib: A 2D graphics environment, Computing in Science & Engineering, 9, 90–95, https://doi.org/10.1109/MCSE.2007.55, 2007.

Iacono, M. J., Delamere, J. S., Mlawer, E. J., Shephard, M. W., Clough, S. A., and Collins, W. D.: Radiative forcing by long-lived greenhouse gases: Calculations with the AER radiative transfer models, J. Geophys. Res.-Atmos., 113, https://doi.org/https://doi.org/10.1029/2008JD009944, 2008.

India Meteorological Department: Frequently Asked Questions (FAQ), http://www.imdsikkim.gov.in/wxfaq.pdf, last access: 30 November 2020.

Jain, S., Sharma, S., Vijayan, N., and Mandal, T.: Seasonal characteristics of aerosols ($PM_{2.5}$ and PM_{10}) and their source apportionment using PMF: A four year study over Delhi, India, Environ. Pollut., p. 114337, https://doi.org/https://doi.org/10.1016/j.envpol.2020.114337, 2020.

Janssens-Maenhout, G., Crippa, M., Guizzardi, D., Dentener, F., Muntean, M., Pouliot, G., Keating, T., Zhang, Q., Kurokawa, J., Wankmüller, R., et al.: HTAP_v2. 2: a mosaic of regional and global emission grid maps for 2008 and 2010 to study hemispheric transport of air pollution, Atmos. Chem. Phys., 15, 11 411–11 432, https://doi.org/https://doi.org/10.5194/acp-15-11411-2015, 2015.

Jethva, H., Satheesh, S., and Srinivasan, J.: Seasonal variability of aerosols over the Indo-Gangetic basin, J. Geophys. Res.-Atmos., 110, https://doi.org/https://doi.org/10.1029/2005JD005938, 2005.

https://doi.org/10.5194/acp-2021-69
Preprint. Discussion started: 4 February 2021


Atmospheric Chemistry and Physics Discussions

Jethva, H., Chand, D., Torres, O., Gupta, P., Lyapustin, A., and Patadia, F.: Agricultural burning and air quality over northern India: a synergistic analysis using NASA's A-train satellite data and ground measurements, Aerosol Air Qual. Res., 18, 1756–1773, https://doi.org/https://doi.org/10.4209/aaqr.2017.12.0583, 2018.

Jethva, H., Torres, O., Field, R. D., Lyapustin, A., Gautam, R., and Kayetha, V.: Connecting crop productivity, residue fires, and air quality over northern India, Sci. Rep., 9, 1–11, https://doi.org/https://doi.org/10.1038/s41598-019-52799-x, 2019.

Knote, C., Hodzic, A., Jimenez, J., Volkamer, R., Orlando, J., Baidar, S., Brioude, J., Fast, J., Gentner, D., Goldstein, A., et al.: Simulation of semi-explicit mechanisms of SOA formation from glyoxal in aerosol in a 3-D model, Atmosf. Chem. Phys., 14, 6213–6239, https://doi.org/https://doi.org/10.5194/acp-14-6213-2014, 2014.

Knote, C., Hodzic, A., and Jimenez, J.: The effect of dry and wet deposition of condensable vapors on secondary organic aerosols concentrations over the continental US., Atmos. Chem. Phys., 15, https://doi.org/https://doi.org/10.5194/acp-15-1-2015, 2015.

Krishna, R. K., Ghude, S. D., Kumar, R., Beig, G., Kulkarni, R., Nivdange, S., and Chate, D.: Surface $PM_{2.5}$ estimate using satellite-derived aerosol optical depth over India, Aerosol Air Qual. Res., 19, 25–37, https://doi.org/https://doi.org/10.4209/aaqr.2017.12.0568, 2019.

Kulkarni, S. H., Ghude, S. D., Jena, C., Karumuri, R. K., Sinha, B., Sinha, V., Kumar, R., Soni, V., and Khare, M.: How Much Does Large-Scale Crop Residue Burning Affect the Air Quality in Delhi?, Environ. Sci. Technol., 54, 4790–4799, https://doi.org/https://doi.org/10.1021/acs.est.0c00329, 2020.

Kumar, M., Tiwari, S., Murari, V., Singh, A., and Banerjee, T.: Wintertime characteristics of aerosols at middle Indo-Gangetic Plain: Impacts of regional meteorology and long range transport, Atmos. Environ., 104, 162–175, https://doi.org/https://doi.org/10.1016/j.atmosenv.2015.01.014, 2015a.

Kumar, M., Parmar, K., Kumar, D., Mhawish, A., Broday, D., Mall, R., and Banerjee, T.: Long-term aerosol climatology over Indo-Gangetic Plain: Trend, prediction and potential source fields, Atmos. Environ., 180, 37–50, https://doi.org/https://doi.org/10.1016/j.atmosenv.2018.02.027, 2018.

Kumar, R., Naja, M., Pfister, G., Barth, M., Wiedinmyer, C., and Brasseur, G.: Simulations over South Asia using the Weather Research and Forecasting model with Chemistry (WRF-Chem): chemistry evaluation and initial results, Geosci. Model Dev., 5, 619, https://doi.org/https://doi.org/10.5194/gmd-5-619-2012, 2012.

Kumar, R., Barth, M., Pfister, G., Nair, V., Ghude, S. D., and Ojha, N.: What controls the seasonal cycle of black carbon aerosols in India?, J. Geophys. Res.-Atmos., 120, 7788–7812, https://doi.org/https://doi.org/10.1002/2015JD023298, 2015b.

Kusaka, H. and Kimura, F.: Coupling a single-layer urban canopy model with a simple atmospheric model: Impact on urban heat island simulation for an idealized case, J. Meteorol. Soc. Jpn., 82, 67–80, https://doi.org/https://doi.org/10.2151/jmsj.82.67, 2004.

Kuttippurath, J., Singh, A., Dash, S., Mallick, N., Clerbaux, C., Van Damme, M., Clarisse, L., Coheur, P.-F., Raj, S., Abbhishek, K., et al.: Record high levels of atmospheric ammonia over India: Spatial and temporal analyses, Sci. Total Environ., p. 139986, https://doi.org/https://doi.org/10.1016/j.scitotenv.2020.139986, 2020.

Lane, T. E., Donahue, N. M., and Pandis, S. N.: Effect of NO x on secondary organic aerosol concentrations, Environ. Sci. Technol., 42, 6022–6027, https://doi.org/https://doi.org/10.1021/es703225a, 2008a.

Lane, T. E., Donahue, N. M., and Pandis, S. N.: Simulating secondary organic aerosol formation using the volatility basis-set approach in a chemical transport model, Atmos. Environ., 42, 7439–7451, https://doi.org/https://doi.org/10.1016/j.atmosenv.2008.06.026, 2008b.

Lelieveld, J., Bourtsoukidis, E., Brühl, C., Fischer, H., Fuchs, H., Harder, H., Hofzumahaus, A., Holland, F., Marno, D., Neumaier, M., et al.: The South Asian monsoon—pollution pump and purifier, Science, 361, 270–273, https://doi.org/https://doi.org/10.1126/science.aar2501, 2018.

https://doi.org/10.5194/acp-2021-69
Preprint. Discussion started: 4 February 2021


Atmospheric Chemistry and Physics Discussions

Levy, R., Mattoo, S., Munchak, L., Remer, L., Sayer, A., Patadia, F., and Hsu, N.: The Collection 6 MODIS aerosol products over land and ocean, Atmos. Meas. Tech., 6, 2989, https://doi.org/https://doi.org/10.5194/amt-6-2989-2013, 2013.

Mallik, C. and Lal, S.: Seasonal characteristics of SO 2, NO 2, and CO emissions in and around the Indo-Gangetic Plain, Environ. Monit Assess., 186, 1295–1310, https://doi.org/https://doi.org/10.1007/s10661-013-3458-y, 2014.

Maussion, F., Siller, M., and Rothenberg, D.: fmaussion/salem: v0.2.1, https://doi.org/10.5281/zenodo.3509134, https://doi.org/10.5281/zenodo.269646, 2017.

Met Office: Cartopy: a cartographic python library with a matplotlib interface, Exeter, Devon, http://scitools.org.uk/cartopy, 2010 - 2015.

Mhawish, A., Banerjee, T., Sorek-Hamer, M., Bilal, M., Lyapustin, A. I., Chatfield, R., and Broday, D. M.: Estimation of High-Resolution $PM_{2.5}$ over the Indo-Gangetic Plain by Fusion of Satellite Data, Meteorology, and Land Use Variables, Environ. Sci. Technol., 54, 7891–7900, https://doi.org/https://doi.org/10.1021/acs.est.0c01769, 2020.

Morrison, H., Curry, J., and Khvorostyanov, V.: A new double-moment microphysics parameterization for application in cloud and climate models. Part I: Description, J. Atmos. Sci., 62, 1665–1677, https://doi.org/https://doi.org/10.1175/JAS3446.1, 2005.

Nakanishi, M. and Niino, H.: An improved Mellor–Yamada level-3 model: Its numerical stability and application to a regional prediction of advection fog, Bound.-Lay. Meteorol., 119, 397–407, https://doi.org/https://doi.org/10.1007/s10546-005-9030-8, 2006.

National Centers for Environmental Prediction, National Weather Service, NOAA, U.S. Department of Commerce: NCEP GDAS/FNL 0.25 Degree Global Tropospheric Analyses and Forecast Grids, https://doi.org/https://doi.org/10.5065/D65Q4T4Z, 2015.

Null, J.: El Niño and La Niña years and intensities, https://ggweather.com/enso/oni.htm, last access: 30 November 2020, 2020.

of Environment Government of Pakistan, M.: Land Use Atlas of Pakistan, Tech. rep., Government of Pakistan, 2009.

Ojha, N., Sharma, A., Kumar, M., Girach, I., Ansari, T. U., Sharma, S. K., Singh, N., Pozzer, A., and Gunthe, S. S.: On the widespread enhancement in fine particulate matter across the Indo-Gangetic Plain towards winter, Sci. Rep., 10, 1–9, https://doi.org/https://doi.org/10.1038/s41598-020-62710-8, 2020.

OpenAQ: Fighting air inequality through open data and community, https://openaq.org/, last access: 30 November 2020.

Pankow, J. F.: An absorption model of gas/particle partitioning of organic compounds in the atmosphere, Atmos. Environ., 28, 185–188, https://doi.org/https://doi.org/10.1016/1352-2310(94)90093-0, 1994.

Pant, P., Shukla, A., Kohl, S. D., Chow, J. C., Watson, J. G., and Harrison, R. M.: Characterization of ambient $PM_{2.5}$ at a pollution hotspot in New Delhi, India and inference of sources, Atmos. Environ., 109, 178–189, https://doi.org/https://doi.org/10.1016/j.atmosenv.2015.02.074, 2015.

Plotly Technologies Inc.: Collaborative data science, https://plot.ly, 2015.

Rajput, P., Sarin, M., Sharma, D., and Singh, D.: Organic aerosols and inorganic species from post-harvest agricultural-waste burning emissions over northern India: impact on mass absorption efficiency of elemental carbon, Environ. Sci-Proc. Imp., 16, 2371–2379, https://doi.org/https://doi.org/10.1039/c4em00307a, 2014.

Ram, K., Sarin, M., and Hegde, P.: Atmospheric abundances of primary and secondary carbonaceous species at two high-altitude sites in India: sources and temporal variability, Atmos. Environ., 42, 6785–6796, https://doi.org/https://doi.org/10.1016/j.atmosenv.2008.05.031, 2008.

Ram, K., Sarin, M., and Tripathi, S.: Temporal trends in atmospheric $PM_{2.5}$, $PM_{2.5}$, elemental carbon, organic carbon, water-soluble organic carbon, and optical properties: impact of biomass burning emissions in the Indo-Gangetic Plain, Environ. Sci. Technol., 46, 686–695, https://doi.org/https://doi.org/10.1021/es202857w, 2012.

https://doi.org/10.5194/acp-2021-69
Preprint. Discussion started: 4 February 2021

Atmospheric Chemistry and Physics Discussions

Reddy, C. S., Pasha, S. V., Jha, C., Diwakar, P., and Dadhwal, V.: Development of national database on long-term deforestation (1930–2014) in Bangladesh, Global Planet. Change, 139, 173–182, https://doi.org/https://doi.org/10.1016/j.gloplacha.2016.02.003, 2016.

Robinson, A. L., Donahue, N. M., Shrivastava, M. K., Weitkamp, E. A., Sage, A. M., Grieshop, A. P., Lane, T. E., Pierce, J. R., and Pandis, S. N.: Rethinking organic aerosols: Semivolatile emissions and photochemical aging, Science, 315, 1259–1262, https://doi.org/https://doi.org/10.1126/science.1133061, 2007.

Schnell, J. L., Naik, V., Horowitz, L. W., Paulot, F., Mao, J., Ginoux, P., Zhao, M., and Ram, K.: Exploring the relationship between surface $PM_{2.5}$ and meteorology in Northern India, Atmos. Chem. Phys., 18, 10 157–10 175, https://doi.org/https://doi.org/10.5194/acp-18-10157-2018, 2018.

Seinfeld, J. H. and Pandis, S. N.: Atmospheric chemistry and physics: from air pollution to climate change, John Wiley & Sons, 2016.

Sembhi, H., Wooster, M., Zhang, T., Sharma, S., Singh, N., Agarwal, S., Boesch, H., Gupta, S., Misra, A., Tripathi, S. N., Mor, S., and Khaiwal, R.: Post-monsoon air quality degradation across Northern India: assessing the impact of policy-related shifts in timing and amount of crop residue burnt, Environ. Res. Lett., 15, 104 067, https://doi.org/10.1088/1748-9326/aba714, 2020.

Shahid, M. Z., Liao, H., Li, J., Shahid, I., Lodhi, A., Mansha, M., et al.: Seasonal variations of aerosols in Pakistan: Contributions of domestic anthropogenic emissions and transboundary transport, Aerosol Air Qual. Res., 15, 1580–1600, https://doi.org/https://doi.org/10.4209/aaqr.2014.12.0332, 2015.

Sharma, S., Mandal, T., Srivastava, M., Chatterjee, A., Jain, S., Saxena, M., Singh, B., Sharma, A., Adak, A., Ghosh, S., et al.: Spatio-temporal variation in chemical characteristics of PM 10 over Indo Gangetic Plain of India, Environ. Sci. and Poll. Res., 23, 18 809–18 822, https://doi.org/10.1007/s11356-016-7025-2, 2016.

Shrivastava, M., Cappa, C. D., Fan, J., Goldstein, A. H., Guenther, A. B., Jimenez, J. L., Kuang, C., Laskin, A., Martin, S. T., Ng, N. L., et al.: Recent advances in understanding secondary organic aerosol: Implications for global climate forcing, Rev. Geophys., 55, 509–559, https://doi.org/https://doi.org/10.1002/2016RG000540, 2017.

Singh, A. P., Singh, R., Mina, U., Singh, M. P., and Varshney, C. K.: Emissions of monoterpene from tropical Indian plant species and assessment of VOC emission from the forest of Haryana state, Atmos. Pollut. Res., 2, 72–79, https://doi.org/https://doi.org/10.5094/APR.2011.009, 2011.

Singh, N., Banerjee, T., Raju, M. P., Deboudt, K., Sorek-Hamer, M., Singh, R. S., and Mall, R. K.: Aerosol chemistry, transport, and climatic implications during extreme biomass burning emissions over the Indo-Gangetic Plain., Atmos. Chem. Phys., 18, https://doi.org/https://doi.org/10.5194/acp-18-14197-2018, 2018.

Srinivas, B. and Sarin, M.: $PM_{2.5}$, EC and OC in atmospheric outflow from the Indo-Gangetic Plain: Temporal variability and aerosol organic carbon-to-organic mass conversion factor, Sci. Total Environ., 487, 196–205, https://doi.org/https://doi.org/10.1016/j.scitotenv.2014.04.002, 2014.

Stavrakou, T., Müller, J.-F., Bauwens, M., De Smedt, I., Van Roozendael, M., Guenther, A., Wild, M., and Xia, X.: Isoprene emissions over Asia 1979-2012: impact of climate and land-use changes, Atmos. Chem. and Phys., 14, 4587–4605, https://doi.org/https://doi.org/10.5194/acp-14-4587-2014, 2014.

Stibig, H.-J., Belward, A., Roy, P., Rosalina-Wasrin, U., Agrawal, S., Joshi, P., Hildanus, Beuchle, R., Fritz, S., Mubareka, S., et al.: A land-cover map for South and Southeast Asia derived from SPOT-VEGETATION data, JJ. Biogeogr., 34, 625–637, https://doi.org/https://doi.org/10.1111/j.1365-2699.2006.01637.x, 2007.

Stone, E., Schauer, J., Quraishi, T. A., and Mahmood, A.: Chemical characterization and source apportionment of fine and coarse particulate matter in Lahore, Pakistan, Atmos. Environ., 44, 1062–1070, https://doi.org/https://doi.org/10.1016/j.atmosenv.2009.12.015, 2010.

https://doi.org/10.5194/acp-2021-69
Preprint. Discussion started: 4 February 2021

Atmospheric Chemistry and Physics Discussions

Surl, L., Palmer, P. I., and González Abad, G.: Which processes drive observed variations of HCHO columns over India?, Atmos. Chem. Phys., 18, 4549–4566, https://doi.org/https://doi.org/10.5194/acp-18-4549-2018, 2018.

The pandas dev. Team: pandas-dev/pandas: Pandas, https://doi.org/10.5281/zenodo.3509134, https://doi.org/10.5281/zenodo.3509134, 2020.

Tie, X., Madronich, S., Walters, S., Zhang, R., Rasch, P., and Collins, W.: Effect of clouds on photolysis and oxidants in the troposphere, J. Geophys. Res.-Atmos., 108, https://doi.org/https://doi.org/10.1029/2003JD003659, 2003.

U.S. Department of State: U.S. Embassy and Consulates' air quality monitors, https://www.airnow.gov/international/us-embassies-and-consulates/, last access: 30 November 2020.

Vadrevu, K. P., Ellicott, E., Badarinath, K., and Vermote, E.: MODIS derived fire characteristics and aerosol optical depth variations during the agricultural residue burning season, north India, Environ. Pollut., 159, 1560–1569, https://doi.org/https://doi.org/10.1016/j.envpol.2011.03.001, 2011.

Venkataraman, C., Brauer, M., Tibrewal, K., Sadavarte, P., Ma, Q., Cohen, A., Chaliyakunnel, S., Frostad, J., Klimont, Z., Martin, R. V., et al.: Source influence on emission pathways and ambient $PM_{2.5}$ pollution over India (2015–2050), Atmos. Chem. Phys., 18, 8017–8039, https://doi.org/https://doi.org/10.5194/acp-18-8017-2018, 2018.

Wang, T., Song, Y., Xu, Z., Liu, M., Xu, T., Liao, W., Yin, L., Cai, X., Kang, L., Zhang, H., et al.: Why is the Indo-Gangetic Plain the region with the largest NH 3 column in the globe during pre-monsoon and monsoon seasons?, Atmos. Chem. Phys., 20, 8727–8736, https://doi.org/https://doi.org/10.5194/acp-20-8727-2020, 2020.

WHO: Ambient air pollution: A global assessment of exposure and burden of disease, Tech. rep., World Health Organization, WHO, 2016.

Wiedinmyer, C., Akagi, S., Yokelson, R. J., Emmons, L., Al-Saadi, J., Orlando, J., and Soja, A.: The Fire INventory from NCAR (FINN): a high resolution global model to estimate the emissions from open burning, Geosci. Model Dev., 4, 625, https://doi.org/https://doi.org/10.5194/gmd-4-625-2011, 2011.

Zaveri, R. A., Easter, R. C., Fast, J. D., and Peters, L. K.: Model for simulating aerosol interactions and chemistry (MOSAIC), J. Geophys. Res.-Atmos., 113, https://doi.org/https://doi.org/10.1029/2007JD008782, 2008.

Zhang, M., Uno, I., Zhang, R., Han, Z., Wang, Z., and Pu, Y.: Evaluation of the Models-3 Community Multi-scale Air Quality (CMAQ) modeling system with observations obtained during the TRACE-P experiment: Comparison of ozone and its related species, Atmos. Environ., 40, 4874–4882, https://doi.org/https://doi.org/10.1002/2017JD027057, 2006.

Zhang, Q., Beekmann, M., Drewnick, F., Freutel, F., Schneider, J., Crippa, M., Prevot, A. S., Baltensperger, U., Poulain, L., Wiedensohler, A., et al.: Formation of organic aerosol in the Paris region during the MEGAPOLI summer campaign: evaluation of the volatility-basis-set approach within the CHIMERE model, Atmos. Chem. Phys., 13, 5767–5790, https://doi.org/https://doi.org/10.5194/acp-13-5767-2013, 2013.

Zhao, B., Wang, S., Donahue, N. M., Jathar, S. H., Huang, X., Wu, W., Hao, J., and Robinson, A. L.: Quantifying the effect of organic aerosol aging and intermediate-volatility emissions on regional-scale aerosol pollution in China, Sci. Rep., 6, 28 815, https://doi.org/https://doi.org/10.1038/srep28815, 2016.